Magmatic development of an intra-oceanic arc: High-precision U-Pb zircon and whole-rock isotopic analyses from the accreted Talkeetna arc, south-central Alaska

Matthew Rioux*
Bradley Hacker
James Mattinson
Department of Earth Science, University of California, Santa Barbara, Santa Barbara, California 93106, USA

Peter Kelemen
Lamont Doherty Earth Observatory, Columbia University, 58 Geochemistry Building, Palisades, New York 10964, USA

Jurek Blusztajn
Department of Geology and Geophysics, Woods Hole Oceanographic Institute, Woods Hole, Massachusetts 02543, USA

George Gehrels
Department of Geosciences, University of Arizona, Tucson, Arizona 85721, USA

ABSTRACT

The accreted Talkeetna arc, south-central Alaska, is an archetypal example of an intra-oceanic arc crustal section. Arc-related units include all levels of a lithospheric column, from residual mantle harzburgites to subaerial volcanic rocks, and provide a rare opportunity to study intrusive arc processes directly. We present the first high-precision U-Pb zircon ages and an extensive new data set of $^{143}Nd/^{144}Nd$ and $^{87}Sr/^{86}Sr$ isotopic analyses from Talkeetna arc plutonic rocks. These data provide new insight into the timing and extent of Talkeetna arc magmatism, the tectonic development of the arc, and the role of preexisting crustal material in the generation of arc magmas. New analyses from the exposed arc crustal section in the Chugach Mountains indicate that the Talkeetna arc began to develop as a juvenile [$\varepsilon_{Nd}(t)$ = 6.0–7.8 and $^{87}Sr/^{86}Sr_{int}$ = 0.703379–0.703951] intra-oceanic arc between 202.1 and 181.4 Ma. This initial arc plutonism was followed ca. 180 Ma by a northward shift in the arc magmatic axis and generation of a large plutonic suite in the Talkeetna Mountains. Plutons from the eastern Talkeetna Mountains yield U-Pb zircon ages of 177.5–168.9 Ma and are isotopically similar to the Chugach Mountains intrusions [$\varepsilon_{Nd}(t)$ = 5.6–7.2 and $^{87}Sr/^{86}Sr_{int}$ = 0.703383–0.703624]. However, plutons from the western Talkeetna Mountains batholith have more evolved initial isotopic ratios [$\varepsilon_{Nd}(t)$ = 4.0–5.5 and $^{87}Sr/^{86}Sr_{int}$ = 0.703656–0.706252] and contain inherited xenocrystic Carboniferous–Triassic zircons. These data are interpreted to represent assimilation of adjacent Wrangellia crust into arc magmas and require amalgamation of the Talkeetna arc with the Wrangellia terrane by ca. 153 Ma. As a whole, the combined U-Pb zircon and isotopic data from the Chugach and Talkeetna Mountains indicate that the main volume of Talkeetna arc magmas formed with little or no involvement of preexisting crustal material. These observations justify the use of the Talkeetna arc as a type section for intrusive intra-oceanic arc crust.

Keywords: island arc, arc plutonism, Talkeetna, Chugach, Alaska, zircon.

INTRODUCTION

Intrusive processes in modern intra-oceanic arcs are largely obscured by the overlying volcanic pile. As a result, studies of arc magmatism rely principally on geochemical trends of volcanic rocks, seismic imaging of active arcs, and the exposure of accreted arc plutonic rocks to understand processes active at depth. The Talkeetna arc, south-central Alaska, includes a faulted cross section from subarc mantle to subaerial volcanic rocks of a Jurassic intra-oceanic arc (Burns, 1985; DeBari and Coleman, 1989), and is considered to be an ideal place to study these processes. Exposures of both the intrusive and extrusive records place direct constraints on geochemical models of magmatic differentiation and provide an important physical analogue for interpreting seismic profiles of modern arcs. The Kohistan arc in Pakistan is the only comparable section on Earth (e.g., Bard, 1983; Treloar et al., 1996; Khan et al., 1997). As a result, the Talkeetna arc has been and continues to be the focus of extensive research on the development and evolution of island arcs (e.g., DeBari and Coleman, 1989; DeBari and Sleep, 1991; Mehl et al., 2003; Kelemen et al., 2003a, 2003b; Rioux et al., 2004; Clift et al., 2005a, 2005b; Greene et al., 2006).

Despite the importance and potential of the Talkeetna arc for understanding intrusive processes in modern arcs, the age and isotopic composition of Talkeetna arc plutonic rocks were poorly constrained. The goals of this study were to determine the timing and extent of Talkeetna arc magmatism, constrain the tectonic evolution of the arc, and determine the role of preexisting crustal material in the generation of the Talkeetna magmas. The results presented herein represent the first high-precision U-Pb zircon ages

*Present address: Department of Earth, Atmospheric and Planetary Sciences, Massachusetts Institute of Technology, Cambridge, MA 02139, USA; riouxm@mit.edu.

GSA Bulletin; September/October 2007; v. 119; no. 9/10; p. 1168–1184; doi: 10.1130B25964.1; 10 figures; 2 tables; Data Repository Item 2007195.

from the Talkeetna arc and an extensive new data set of $^{143}Nd/^{144}Nd$ and $^{87}Sr/^{86}Sr$ analyses.

GEOLOGY OF THE TALKEETNA ARC

The Talkeetna arc is exposed as one of a series of accreted terranes along the southern margin of Alaska. The volcanic carapace of the arc and overlying sedimentary sequences define the extent of the Jurassic Peninsular terrane (Jones and Silberling, 1979), which is composed of four major volcanic and plutonic sections in the Chugach Mountains, the Talkeetna Mountains, Kodiak Island, and the Alaska Peninsula (Fig. 1; e.g., Reed and Lanphere, 1973; Hudson, 1979; Pavlis, 1983; Burns, 1985; Hudson et al., 1985). In the northern Talkeetna Mountains, the Peninsular terrane is juxtaposed with the allochthonous Wrangellia terrane, an extensive Triassic oceanic flood basalt erupted over an existing Paleozoic arc sequence and subsequently intruded by a Jurassic intra-oceanic volcanic arc (Bond, 1973; Richter and Jones, 1973; Nokleberg et al., 1985, 1994; Barker et al., 1994; DeBari et al., 1999). Overlap assemblages suggest that the Peninsular and Wrangellia terranes either formed as a single tectonic block or were merged into a composite terrane prior to accretion onto the North American margin (Plafker et al., 1989; Nokleberg et al., 1994); however, the timing of terrane juxtaposition and subsequent accretion are subjects of ongoing research (e.g., Plafker et al., 1989; McClelland et al., 1992; Gehrels, 2001; Ridgway et al., 2002; Trop et al., 2002, 2005). To the south, the Peninsular terrane is bounded by the regional Border Ranges fault, which places Talkeetna arc plutonic and volcanic rocks in contact with synchronous and younger accretionary complexes of the Chugach terrane (Fig. 2; Sisson and Onstott, 1986; Pavlis et al., 1988; Roeske et al., 1989; Clift et al., 2005b).

This contribution concentrates on the evolution of arc plutonism in the Chugach and Talkeetna Mountains. In the Chugach Mountains, the exposed volcanic and plutonic lithologies preserve a complete cross section from the subarc mantle to the volcanic carapace of the arc (Burns, 1985; DeBari and Coleman, 1989). The lowest units in the arc are exposed directly north of the Border Ranges fault and preserve the transition from residual mantle harzburgite-dunite to cumulate pyroxenite (i.e., the petrologic Moho; DeBari and Coleman, 1989). These lithologies grade upsection into extensive lower and mid-crustal gabbronorites and intermediate to felsic plutonic rocks (Burns, 1985; DeBari and Coleman, 1989) that are exposed in the main arc section north of the Border Ranges fault and within a single klippe of arc crust south of the fault in the Klanelneechena area (Fig. 2). The timing of emplacement of the Klanelneechena klippe is unknown, but Early Jurassic U-Pb ages (this study), arc-like geochemical signatures (Kelemen et al., 2003a), mid-crustal pressures (0.7 GPa; Hacker et al., 2005), and proximity to arc exposures north of the Border Ranges fault (Winkler et al., 1981) are consistent with the klippe representing a faulted block of mid-crustal intrusive rocks from the Talkeetna arc. The volcanic carapace of the arc is preserved as the Jurassic Talkeetna Formation, ~7 km of submarine and subaerial lava, tuff, ignimbrite, and volcaniclastic deposits (Clift et al., 2005a). Thermobarometry from a thin layer (~500 m) of garnet gabbronorite directly above the Moho records metamorphic pressure-temperature conditions of 0.9–1.0 GPa and ~875–935 ºC (Mehl et al., 2001; Kelemen et al., 2003b; Hacker et al., 2005) and indicates an original arc crustal thickness of ~30 km; however, the entire arc section has been dissected and thinned by significant postmagmatic faulting.

In the Talkeetna Mountains, intermediate to felsic plutons intrude northern exposures of the Talkeetna Formation (Fig. 2). The series of elongate NE-SW-trending plutons range from quartz diorite to trondhjemite and have typical arc geochemistry (Rioux et al., 2004). The plutonic rocks have been interpreted to represent both a distinct magmatic arc (Hudson, 1979) and an extension of Talkeetna arc magmatism (Pavlis, 1983; Hudson et al., 1985). An important goal of this paper is to define the temporal and genetic relationship of the Talkeetna Mountains plutons to the arc section in the Chugach Mountains.

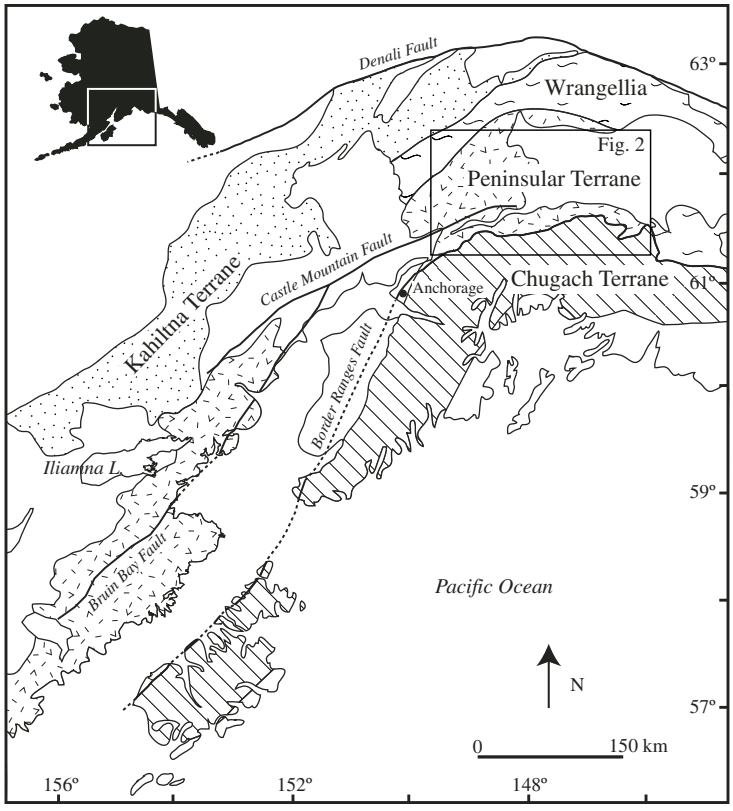

Figure 1. Terrane map of south-central Alaska (after Silberling et al., 1994). The Peninsular terrane is defined by the extent of Talkeetna arc volcanic rocks and the overlying sedimentary section (Jones and Silberling, 1979).

ANALYTICAL METHODS

High-precision U-Pb zircon ages for this study were determined using the chemical abrasion–thermal ionization mass spectrometry (CA-TIMS) technique of Mattinson (2003, 2005a). This method combines annealing and multistage digestion to analyze a zircon population. High-temperature annealing (800–1000 ºC) is used to repair radiation damage in individual crystals and to prevent chemical leaching of radiogenic Pb during the multistage analyses (e.g., Mattinson, 1994). The annealed population is then dissolved in two or more steps by varying digestions times and temperatures. Observation of partially dissolved zircon populations reveals

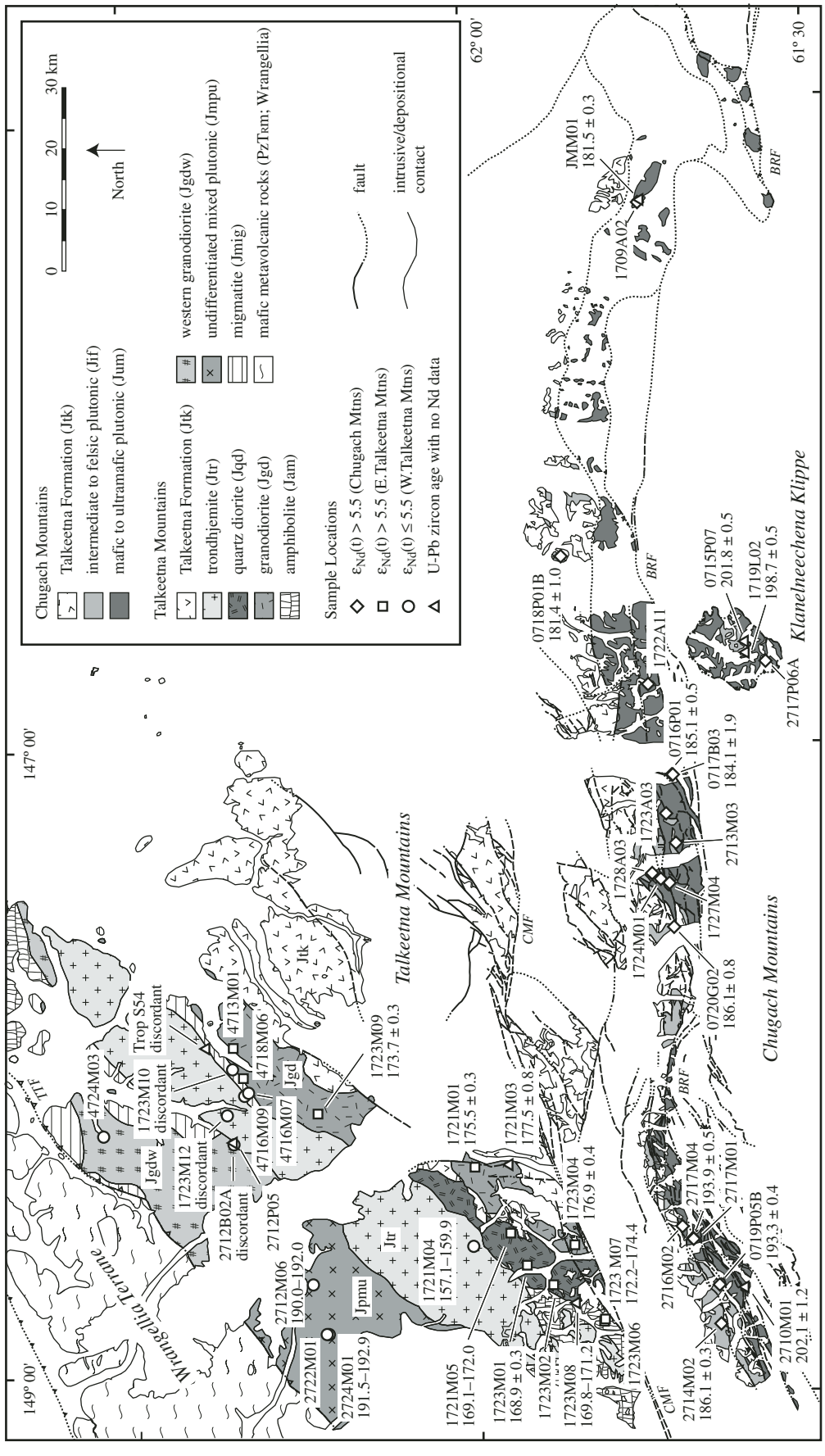

Figure 2. Geologic map of the Chugach and Talkeetna Mountains showing sample locations (Table 1) and the spatial distribution of the chemical abrasion–thermal ionization mass spectrometry U-Pb zircon ages and radiogenic isotope data reported herein. BRF—Border Ranges fault; CMF—Castle Mountain fault; TTF—Talkeetna thrust fault. The geologic map is modified from Csejtey et al. (1978), Winkler et al. (1981), Winkler (1992), and Wilson et al. (1998).

that some grains dissolve sequentially from rim to core while others are infiltrated by acid along preexisting cracks or soluble layers (Figs. 3B, 3C). Chemical analyses of the leachates indicate that initial digestion steps remove material with higher concentrations of U and other chemical impurities (e.g., Th, Y, rare earth elements [REE]). These layers are the most susceptible to radiation damage due to the decay of U and Th and typically record evidence for secondary Pb loss (Fig. 3A). Further research is necessary to determine what leads to the differential solubility of zircon in the multistep analyses; however, the higher concentration of trace elements in more soluble layers suggests that the effect may be related to either an increase in the strain free energy of the lattice or to residual effects from radiation damage in the U- and Th-rich layers (Mattinson, 2005a). Multigrain and single-grain studies have demonstrated that chemical abrasion has the ability to remove disturbed zircon lattice that is inaccessible to traditional pretreatments (e.g., physical abrasion), and therefore provides more precise and accurate ages (e.g., Mattinson, 1994, 2005a; McClelland and Mattinson, 1996; Mundil et al., 2004).

TABLE 1. SAMPLE LOCATIONS AND ROCK TYPES

Sample	UTM (E)†	UTM (N)†	Rock type‡
Chugach Mountains			
JMM 01	0589390	6846813	pegmatite
0715P07	0516804	6831035	trondhjemite
0716P01	0495095	6843558	trondhjemite
0717B03	0495060	6843454	trondhjemite
0718P01B	0531175	6860727	trondhjemite
0719P05B	0410838	6837116	trondhjemite
0720G02	0469477	6843396	quartz diorite
1709A02	0588877	6847320	gabbronorite
1719L02	0514744	6831007	garnet gabbro
1722A11	0510122	6846862	gabbronorite
1723A03	0488891	6844348	gabbronorite
1724M01	0477760	6845355	quartz diorite
1727M04	0477167	6844075	quartz diorite
1728A03	0478732	6846830	mafic dike
2710M01	0410370	6833285	metavolcanic/ clastic
2713M03	0483535	6842885	gabbro
2714M02	0404764	6836991	tonalite
2716M02	0420424	6843102	quartz diorite
2717M01	0418768	6841304	diorite
2717M04	0418800	6841169	diorite
2717P06A	0513359	6827773	garnet trondhjemite
Eastern Talkeetna Mountains			
1721M01	0430974	6876836	granodiorite
1721M03	0430566	6870852	granodiorite
1721M05	0419863	6871256	quartz diorite
1723M01	0414618	6868471	quartz diorite
1723M02	0411233	6864264	quartz diorite
1723M04	0417960	6860699	granodiorite
1723M06	0405233	6856125	amphibolite
1723M07	0405511	6856079	quartz diorite
1723M08	0408019	6860756	quartz diorite
1723M09	0440158	6902343	granodiorite
4713M01	0451121	6915756	granodiorite
4718M06	0446142	6914209	granodiorite
Western Talkeetna Mountains			
TropS54	0451107	6920052	trondhjemite
1721M04	0418246	6876922	trondhjemite
1723M10	0447622	6915897	trondhjemite
1723M12	0440230	6916915	trondhjemite
2712B02A	0435108	6916127	tonalite
2712M06	0411553	6903246	tonalite
2712P05	0434615	6915929	amphibolite
2722M01	0402870	6901919	amphibolite
2724M01	0403861	6901169	tonalite
4716M07	0443744	6913385	metavolcanic
4716M09	0443284	6914009	trondhjemite
4724M03	0437043	6937156	granodiorite

†UTM (Universal Transverse Mercator) coordinates are relative to the North American Datum 27. All points are in the 06 UTM zone.
‡Igneous rock types follow Streckeisen (1973, 1976) and Le Maitre et al. (2002).

Multistep CA-TIMS analyses for this study were carried out at the University of California, Santa Barbara (UCSB). Zircon concentrates were generated by standard magnetic and density separation techniques. Analyzed zircon populations were hand-picked from the least magnetic fractions, with the exception of sample 1723M10, where zircons were concentrated in the final magnetic fraction (150 V, 8º tilt on a Frantz magnetic separator). For each sample, one multigrain zircon fraction (0.2–24.2 mg) was annealed at 850–1000 ºC for 48 h and then dissolved in 4–14 discrete steps (see GSA Data Repository Table DR1[1]). The number of digestion steps depended on the size of the sample, the solubility of the zircons, and the digestion temperatures. All digestions were done in Teflon capsules within Parr bombs using 10 parts 50% HF to one part 8 N HNO_3 and a combined ^{205}Pb-^{235}U tracer. Following each digestion step, the samples were dried on a hot plate and redissolved in 3.1 N HCl in the oven at 140 ºC for 12–20 h. After removing the sample solution, the remaining grains were rinsed 2–3 times with 3.1 N HCl and returned to the oven in 3.1 N HCl at 170 ºC for 20 h. The clean-up procedure was repeated twice between each digestion step to avoid cross contamination. Uranium and Pb were separated using standard ion-exchange columns miniaturized after Krogh (1973), and analyzed on the multicollector Finnigan MAT-261 at UCSB. Isotopic ratios were measured using Faraday cups in static collection mode with simultaneous measurement of ^{204}Pb on a Spectromat ion-counting system. The results of the multigrain analyses are plotted on Tera-Wasserberg concordia and $^{206}Pb/^{238}U$ release diagrams in Figures 4–6.

[1]GSA Data Repository Item 2007195, Tables DR1–DR3, TIMS and LA-ICP-MS U-Pb data tables, is available at www.geosociety.org/pubs/ft2007.htm. Requests may also be sent to editing@geosociety.org.

In addition to the multigrain analyses, limited single-grain chemical abrasion analyses were carried out at the Massachusetts Institute of Technology (MIT) (Table DR2; see footnote 1). For these experiments individual zircons were subjected to a single 12–16 h, 180 ºC leach followed by rinsing and a 2 day final digestion at 220 ºC. Analytical procedures for the single-grain analyses follow Schoene et al. (2006). A discussion of U-Pb zircon error analysis and analytical details for laser ablation-inductively coupled plasma-mass spectrometry (LA-ICP-MS) U-Pb zircon dating and whole-rock isotopic analyses are provided in the Appendix.

RESULTS

U-Pb Zircon Dating

To illuminate the timing and evolution of Talkeetna arc magmatism, we measured U-Pb zircon ages from 25 samples from the Chugach and Talkeetna Mountains. Sample locations and rock types are listed in Table 1. Ten samples from the Chugach Mountains define concordant or near-concordant ages between 202.1 ± 1.2 Ma and 181.4 ± 1.0 Ma (Fig. 4). Chemical-abrasion data from seven of these (0718P01B, JMM01, 0717B03, 0720G02, 2714M02, 0719P05B, and 2717M04) have digestion patterns typical of homogeneous zircon populations: low-temperature digestion steps have young $^{206}Pb/^{238}U$ ages, as a result of geologic Pb loss, and higher temperature steps are concordant (or nearly concordant) and overlap within error (Figs. 4A–4G). For these analyses, we interpret the weighted mean of the concordant and equivalent $^{206}Pb/^{238}U$ data as the crystallization age of the sample (181.4 ± 1.0 Ma, 181.5 ± 0.3 Ma, 184.1 ± 1.9 Ma, 186.1 ± 0.8 Ma, 186.1 ± 0.3 Ma, 193.3 ± 0.4 Ma, 193.9 ± 0.5 Ma; all weighted mean errors are reported at the 95% confidence interval). We excluded the residue step from sample 2717M04 because it has an anomalously high $^{207}Pb/^{206}Pb$ age that is most likely an analytical artifact. The high mean square of weighted deviates (MSWD) value for sample 0718P01B indicates that the scatter in the data is not fully explained by the analytical errors (Fig. 4A). The MSWD of the other analyses are within the 2σ range of expected values (i.e., MSWD = 1 ± 2σ) outlined by Wendt and Carl (1991).

Three additional samples from the Chugach Mountains merit a more detailed discussion (0716P01, 0715P07, and 1719L02; Figs. 4H–4J). All three analyses generated typical chemical abrasion patterns—low-temperature digestions steps are discordant and have increasing $^{206}Pb/^{238}U$ ages with increasing digestion temperature—but yielded only a single concor-

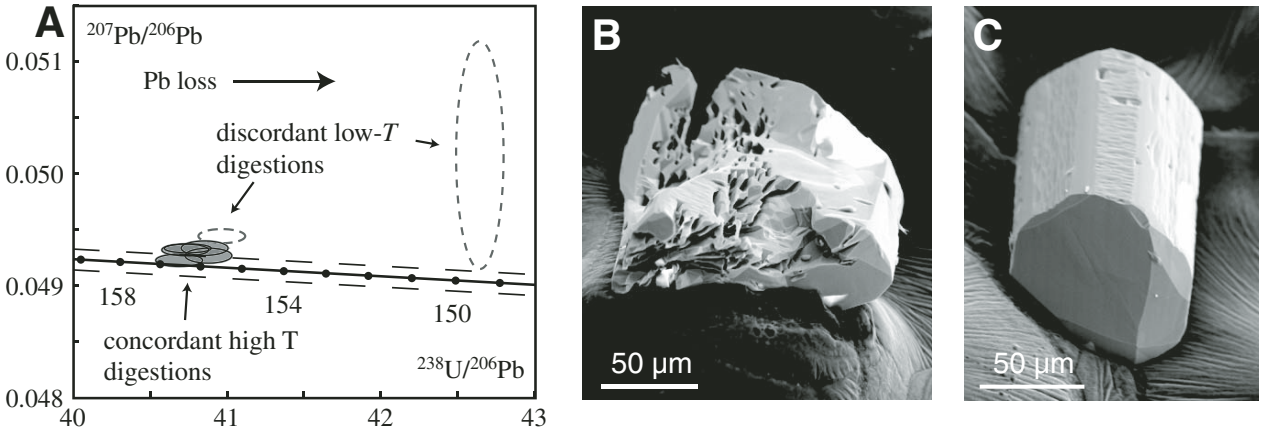

Figure 3. (A) Chemical abrasion–thermal ionization mass spectrometry results from a homogeneous zircon population (Trop et al., 2005). Low-temperature (*T*) digestion steps removed disturbed material affected by secondary Pb loss. Dashed lines show decay-constant errors on concordia. (B, C) Scanning electron microscope images of two grains that were annealed and partially dissolved under the same conditions but show distinct digestion patterns. The zircons are from a Cretaceous pluton in the Sierra Nevada batholith, California.

dant high-temperature digestion step. For samples 0716P01 and 0715P07, the ^{206}Pb/^{238}U ages of the two final steps overlap within error; however, the D step for sample 0716P01 is poorly constrained as a result of analytical difficulties and the C step for sample 0715P07 is slightly discordant. In all three analyses the residue step made up a significant portion (37%–90%) of the total zircon. For these samples we interpret the concordant residue step as the crystallization age of the sample (185.1 ± 0.5 Ma, 201.8 ± 0.5 Ma, and 198.7 ± 0.5 Ma); however, the absence of multistep ^{206}Pb/^{238}U age plateaus in the analyses strictly precludes assessment of minor Pb loss or inheritance in the final digestion at a level too subtle for detection by classic discordance between the ^{206}Pb/^{238}U and ^{207}Pb/^{206}Pb ages.

A single sample from the Chugach Mountains (2710M01) was dated by single-grain U-Pb zircon analyses at MIT (Table DR2; see footnote 1). Data from this sample define two distinct populations with weighted mean ^{206}Pb/^{238}U ages of 202.1 ± 1.2 Ma (n = 3, MSWD = 2.6) and 205.8 ± 0.4 Ma (n = 3, MSWD = 0.9). The data are consistent with inheritance of 205.8 Ma zircons into a 202.1 Ma magma.

Plutons from the Talkeetna Mountains have a range of chemical-abrasion patterns that follow distinct geographic trends (Figs. 5 and 6). Four samples from a granodiorite pluton (Jgd; 1723M09, 1721M01, 1723M04, and 1721M03) along the eastern margin of the batholith (Fig. 2) record concordant crystallization ages of 173.7 ± 0.3 Ma, 175.5 ± 0.3 Ma, 176.9 ± 0.4 Ma, and 177.5 ± 0.8 Ma (Figs. 5A–5D). The MSWDs for these data are within the expected range (Wendt and Carl, 1991). In contrast, data from an adjacent quartz diorite pluton have complex digestion patterns that reflect a range of zircon systematics. A single analysis (1723M01) from the pluton generated a simple multistep crystallization age of 168.9 ± 0.3 Ma (MSWD = 1.0; Fig. 5E), whereas three additional samples (1721M05, 1723M07, and 1723M08) define 1.4–2.9 m.y. spreads along concordia with an increase in ^{206}Pb/^{238}U ages from successive digestion steps (Figs. 5F–5H). The spread in the data is consistent with either pervasive Pb loss or minor inheritance of older zircon. However, we prefer the latter explanation because detailed chemical abrasion experiments demonstrate that low-temperature digestion steps in the multistep technique effectively eliminate measurable Pb loss in low-U zircons (e.g., Mundil et al., 2004; Mattinson, 2005a; this study). Following this interpretation, once the initial steps have removed the effects of Pb loss, the remaining steps represent mixing between newly crystallized igneous zircon and a very slightly older inherited component. The lower limit of the age range in Figure 5 is then a maximum crystallization age for the sample, and the upper end of the range is a minimum age for the inherited component. The LA-ICP-MS analyses from the three samples define near-Gaussian ^{206}Pb/^{238}U age distributions (n ~ 50 for each sample; Figs. 7A–7C), indicating that any inherited component has an age within the ~30–60 m.y. scatter of the data. Cathodoluminescence images of the grains do not show obvious cores or rims, but this may reflect overgrowth of chemically similar zircon. Weighted mean ^{206}Pb/^{238}U ages of the laser analyses (168.9 ± 3.3 Ma, 169.4 ± 1.5 Ma, and 168.3 ± 1.8 Ma) agree well with the crystallization age for sample 1723M01 (168.9 ± 0.3 Ma).

A trondhjemite pluton from the center of the Talkeetna Mountains records the youngest ages in the Jurassic section. Sample 1721M04 has a spread of data that parallels concordia, with a monotonic increase in the ^{206}Pb/^{238}U ages from 157.1 to 159.9 Ma (Fig. 6A). As with the data described above, LA-ICP-MS spot analyses from this sample (n = 44) do not show a significantly older inherited component, so we interpret the spread in the ages as mixing between two populations of similarly aged Jurassic zircons. Two samples (1723M12 and Trop S54) from more northern exposures of the trondhjemite have variable and discordant ages that define U-shaped ^{206}Pb/^{238}U release patterns (Figs. 6B, 6C). The initial decline in the ^{206}Pb/^{238}U ages is similar to the digestion patterns of zircon populations with a large inherited component, and we attribute the U-shaped patterns to differential digestion of a zircon population with younger overgrowths on older cores. As discussed above, observations of partially dissolved zircon populations suggest that some grains dissolve sequentially from rim to core, whereas others are infiltrated by the acid. The U-shaped digestion patterns may reflect this bimodal digestion, wherein some older cores were mined out during the initial steps (e.g., McClelland and Mattinson, 1996) and others were protected by nonmetamict younger rims until later digestions. The youngest ^{206}Pb/^{238}U age (155.0 ± 0.7 Ma), excluding the initial A clean-up steps, represents a maximum age for crystallization of the trondhjemite. The LA-ICP-MS spot analyses from sample 1723M12 (n = 47; Fig. 7F) record

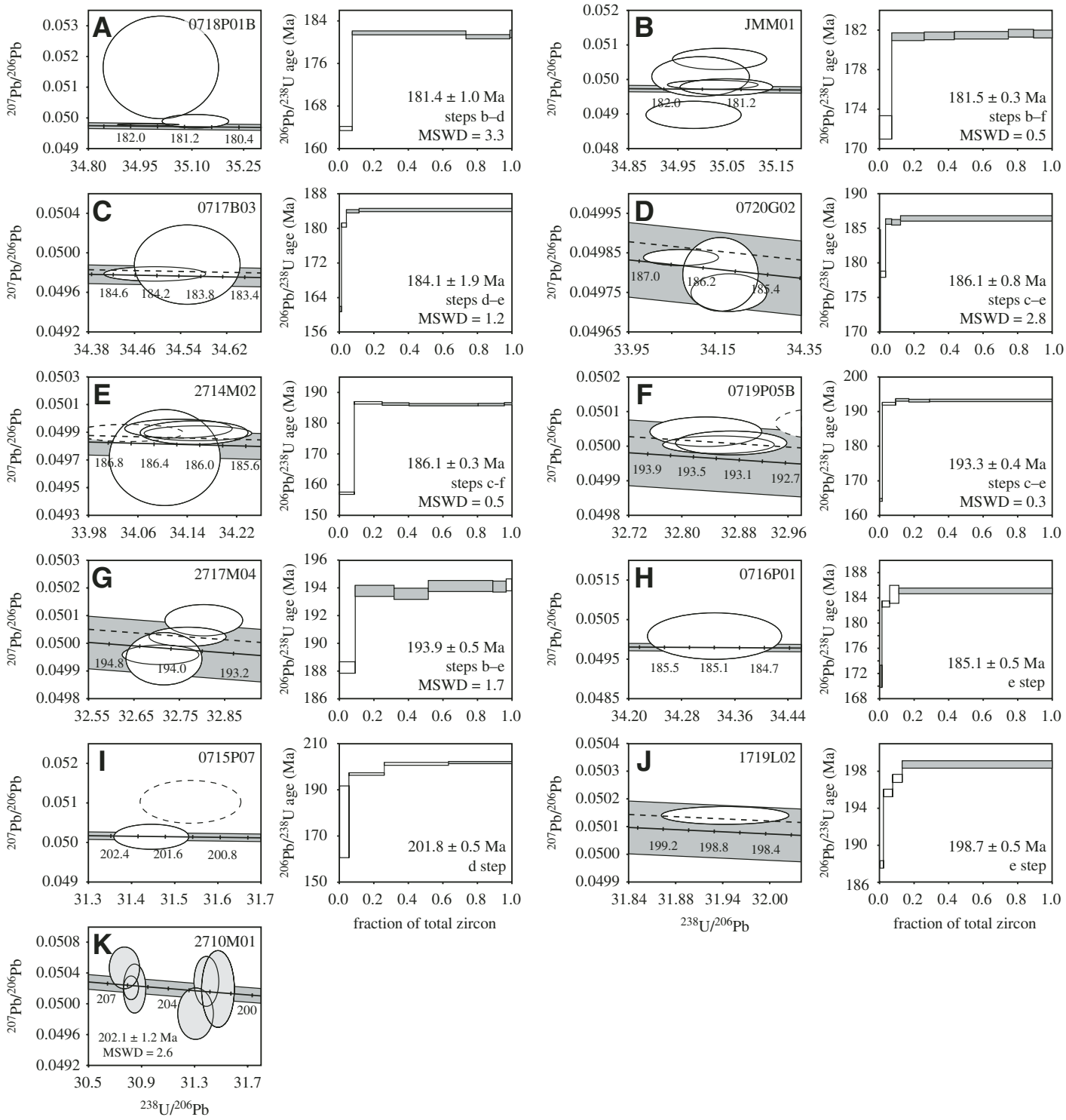

Figure 4. Tera-Wasserburg concordia plots and zircon-digestion diagrams for chemical abrasion–thermal ionization mass spectrometry data from the Chugach Mountains. Plots A–J represent multistep analyses of zircon populations. Plot K shows the final digestion step for six single-grain chemical abrasion analyses (shaded ellipses). The data from the Chugach Mountains are typically concordant or near concordant and record $^{206}Pb/^{238}U$ ages from 202.1 to 181.4 Ma. The digestion diagrams plot $^{206}Pb/^{238}U$ ages versus the fraction of total zircon dissolved in each digestion step, progressing from low- to high-temperature digestion steps. Solid white error ellipses correspond to the shaded steps in the digestion diagrams. For samples with reported $^{206}Pb/^{238}U$ ages, the shaded data were used to calculate the sample age. All error ellipses are 2σ. The gray band on concordia shows 2σ uncertainties based on decay-constant uncertainties of ^{238}U = 0.107% and ^{235}U = 0.136% (Jaffey et al., 1971). The dashed line shows the revised concordia of Mattinson (2000) and Schoene et al. (2006; see Appendix). MSWD—mean square of weighted deviates. Ages along concordia are in Ma. All plots were produced using Isoplot 3.0/3.2 (Ludwig, 2003). Analytical details and raw data are in Tables DR1 and DR2 (see footnote 1).

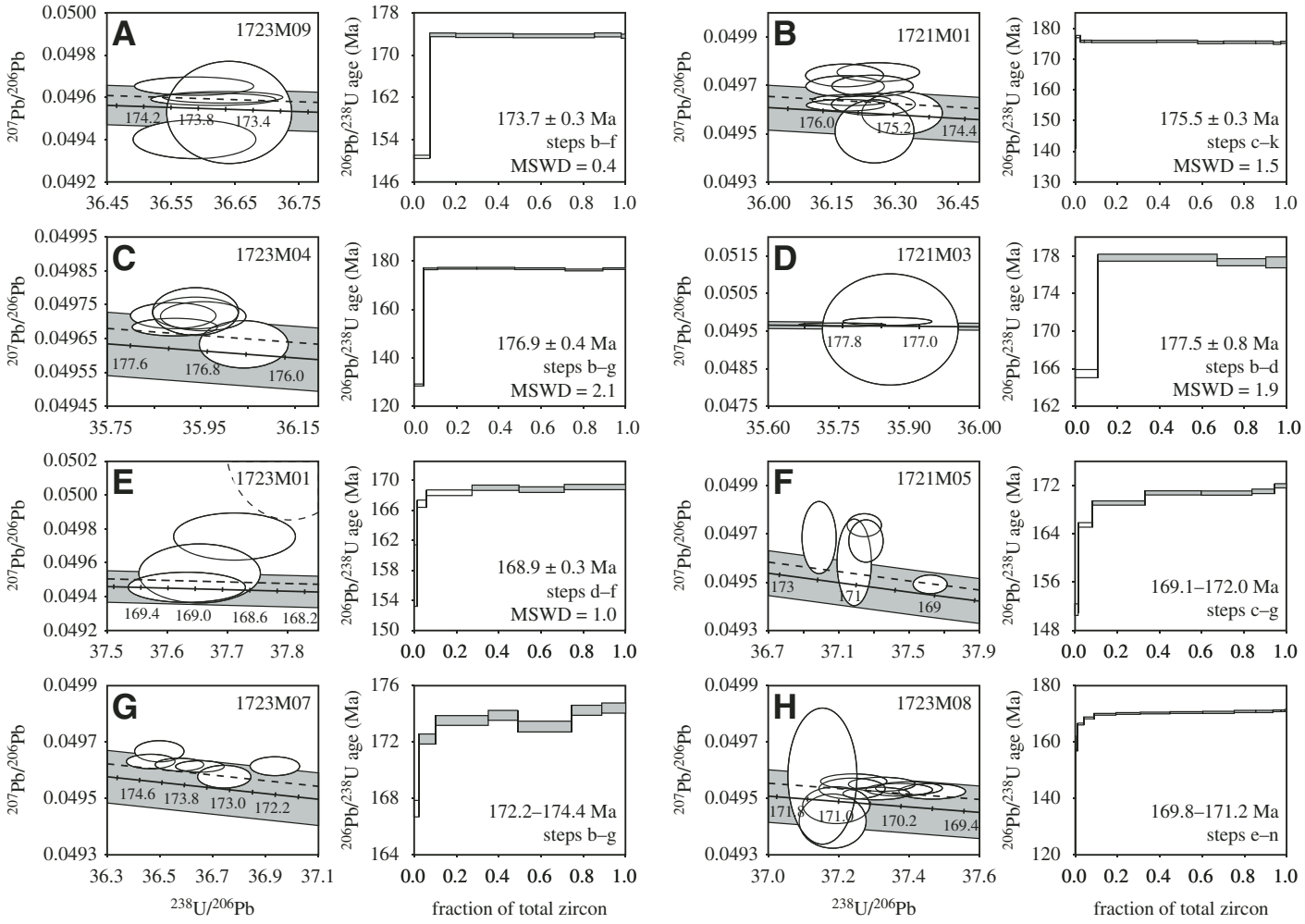

Figure 5. Tera-Wasserburg concordia plots and zircon-digestion diagrams for chemical abrasion–thermal ionization mass spectrometry data from the eastern Talkeetna Mountains. The data define two distinct digestion patterns. High-temperature digestion steps from samples 1723M09, 1721M01, 1723M04, 1721M03, and 1723M01 are concordant and overlap within error, defining $^{206}Pb/^{238}U$ ages from 177.5 to 168.9 Ma. In contrast, step analyses from samples 1721M05, 1723M07, and 1723M08 spread along concordia. These digestion patterns and laser ablation-inductively coupled plasma-mass spectrometry spot analyses from these samples (Fig. 7) are consistent with minor inheritance of Mesozoic zircon. MSWD—mean square of weighted deviates. Plot details are described in Figure 4.

a cluster of ages ca. 156 Ma with limited older ages to 320 Ma, confirming the presence of the inherited component implied by the CA-TIMS analyses. In contrast, the laser data from Trop S54 define a single homogeneous population with a $^{206}Pb/^{238}U$ age of 152.7 ± 1.3 Ma (n = 89; MSWD = 0.9; Fig. 7E). The absence of an inherited signature in the latter analyses may reflect the finer grain size of the zircon we analyzed by LA-ICP-MS. We interpret the weighted mean $^{206}Pb/^{238}U$ age of the LA-ICP-MS spot analyses as the crystallization age for this sample.

A single sample (1723M10; Fig. 6D) from a migmatite along the eastern margin of the trondhjemite generated discordant analyses that record more extensive evidence of inherited older material. The zircons from this sample have high U concentrations (1500–2500 ppm) and most appear to be metamict. The zircons dissolved completely in the first two steps of the chemical-abrasion analysis and were most likely affected by extensive geologic Pb loss. A tie line between the residue step and modern Pb loss generates a concordia intercept age of ca. 300 Ma and requires a Paleozoic or older inherited component in the sample. A mixing line between the ca. 153 Ma intrusion age of the trondhjemite pluton and the higher temperature digestion step is consistent with the Carboniferous inheritance seen in other samples from this area.

The western margin of the Talkeetna Mountain batholith is composed of Early Jurassic plutons that contain additional evidence for inheritance of Paleozoic zircon. Mapped units in this area include a large granodioritic pluton (Jgdw) and a unit of intermingled plutonic lithologies (Jpmu; Fig. 2; Csejtey et al., 1978). A single sample from the granodiorite (2712B02A) yielded highly discordant TIMS data (Fig. 6E). Five LA-ICP-MS spot analyses from the same sample produced a cluster of data at 190.5 ± 6.8 Ma (n = 4; MSWD = 0.4) and a single older spot with a $^{206}Pb/^{238}U$ age of 275.3 ± 12.0 Ma (individual spot errors are 2σ; Fig. 7G). Two samples from tonalite (2724M01) and quartz diorite (2712M06) intrusions within the intermingled plutons generated a spread of concordant analyses with Early Jurassic $^{206}Pb/^{238}U$ ages (192.9–191.5 Ma and 192.0–190.0 Ma; Figs. 6F, 6G) and LA-ICP-MS analyses from these samples record evidence of

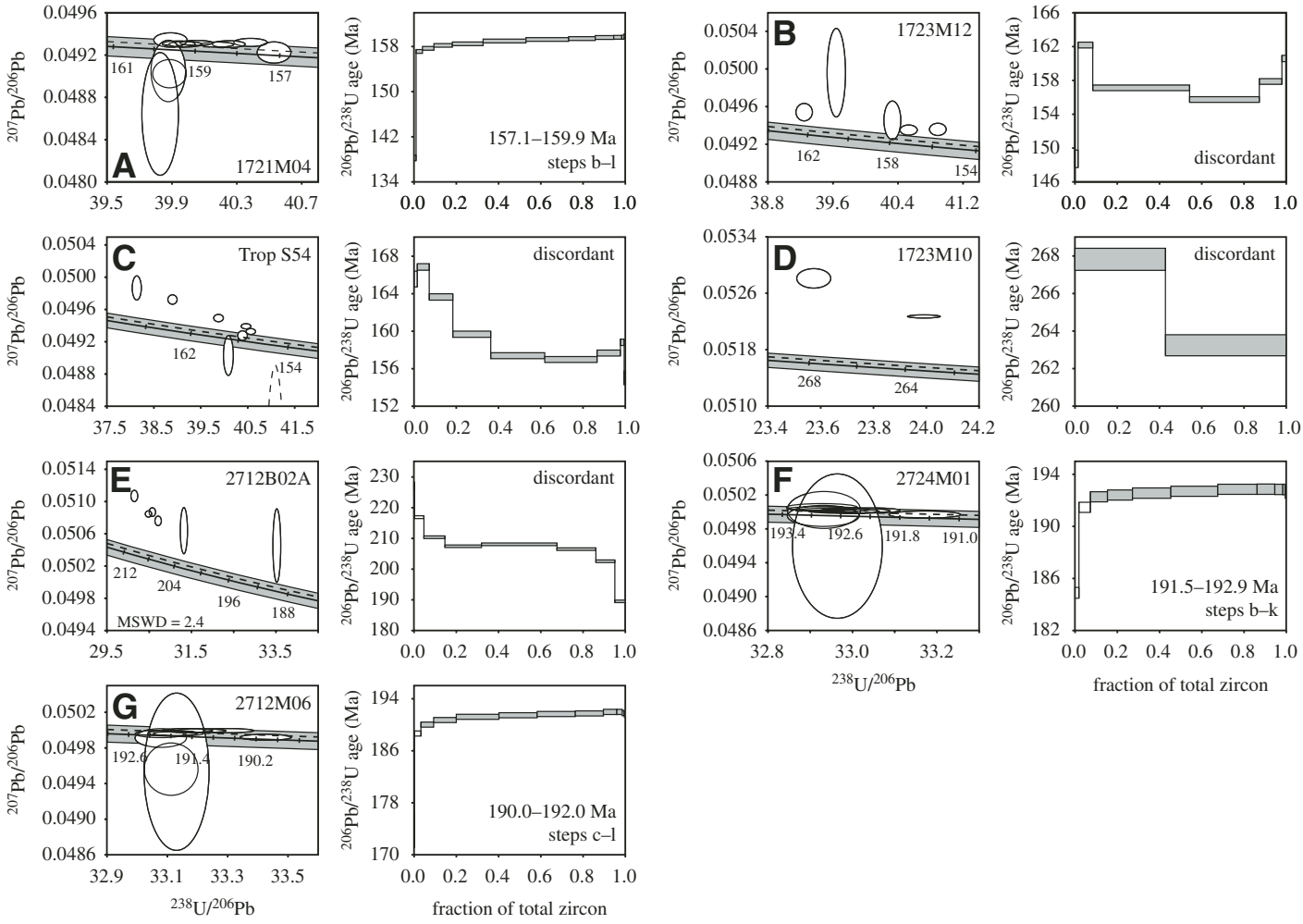

Figure 6. Tera-Wasserburg concordia plots and zircon-digestion diagrams for chemical abrasion–thermal ionization mass spectrometry data from the central and western Talkeetna Mountains. The data are either discordant or define a spread of ages along concordia. The digestion patterns and laser ablation-inductively coupled plasma-mass spectrometry (LA-ICP-MS) spot analyses from these samples, excluding 1721M04, reflect inheritance of Triassic–Carboniferous zircons into 191–153 Ma magmas. The digestion patterns and LA-ICP-MS analyses for 1721M04 are consistent with either minor Mesozoic inheritance or pervasive Pb loss. Plot details are described in Figure 4.

Paleozoic xenocrysts. Spot analyses from sample 2724M01 generated an asymmetric cluster of ages with a weighted mean $^{206}Pb/^{238}U$ age of 187.4 ± 2.2 Ma (n = 44; MSWD = 2.0) and two outlying data with $^{206}Pb/^{238}U$ ages of 232.0 ± 17.0 Ma and 290.1 ± 22.8 Ma (Fig. 7H). Data from sample 2712M06 form a single asymmetric distribution with a weighted mean $^{206}Pb/^{238}U$ age of 191.1 ± 3.4 Ma (n = 44; MSWD = 5.0) and a maximum spot age of 226.3 ± 7.6 Ma (Fig. 7I). We therefore interpret the chemical-abrasion and laser-ablation analyses to reflect mixing between Early Jurassic magmatic zircon and inherited late Carboniferous–Triassic material. The absence of a U-shaped digestion pattern in the chemical abrasion data suggests that the inherited zircons—which the LA-ICP-MS analyses indicate made up a minor component of the entire zircon population—were either chemically similar to the younger arc zircons or were shielded by coherent younger rims and were therefore not preferentially dissolved during early digestion steps.

Radiogenic Isotope Tracers

Radiogenic isotope data complement the U-Pb zircon analyses and provide information on the composition of the source and the role of crustal contamination in Talkeetna arc magmatism. Age-corrected $^{143}Nd/^{144}Nd$ and $^{87}Sr/^{86}Sr$ ratios from the Chugach Mountains define a restricted array of initial isotopic ratios [$\varepsilon_{Nd}(t)$ = 6.0–7.8 and $^{87}Sr/^{86}Sr_{int}$ = 0.703379–0.703951; Fig. 8] consistent with the absence of inherited zircon in this region. Our new data agree with published Nd data from the Talkeetna Formation volcanic rocks and Chugach Mountain plutons (Clift et al., 2005a; Greene et al., 2006). In contrast, age-corrected ratios from the Talkeetna Mountains define two distinct isotopic domains: samples from the eastern Talkeetna Mountains (Jgd and Jqd; Fig. 2) are characterized by isotopic ratios that are indistinguishable from the Chugach data [$\varepsilon_{Nd}(t)$ = 5.6–7.2 and $^{87}Sr/^{86}Sr_{int}$ = 0.703383–0.703624], whereas samples from the western intrusions (Jtr, Jpmu, and Jgdw; Fig. 2) have lower $^{143}Nd/^{144}Nd$ ratios and elevated $^{87}Sr/^{86}Sr$ ratios [$\varepsilon_{Nd}(t)$ = 4.0–5.5 and $^{87}Sr/^{86}Sr_{int}$ = 0.703656–0.706252] indicating a distinct source or contamination by an enriched and/or older crustal component with low $^{143}Nd/^{144}Nd$ and high $^{87}Sr/^{86}Sr$. A single analysis from an undated metavolcanic wall rock (4716M07) along the

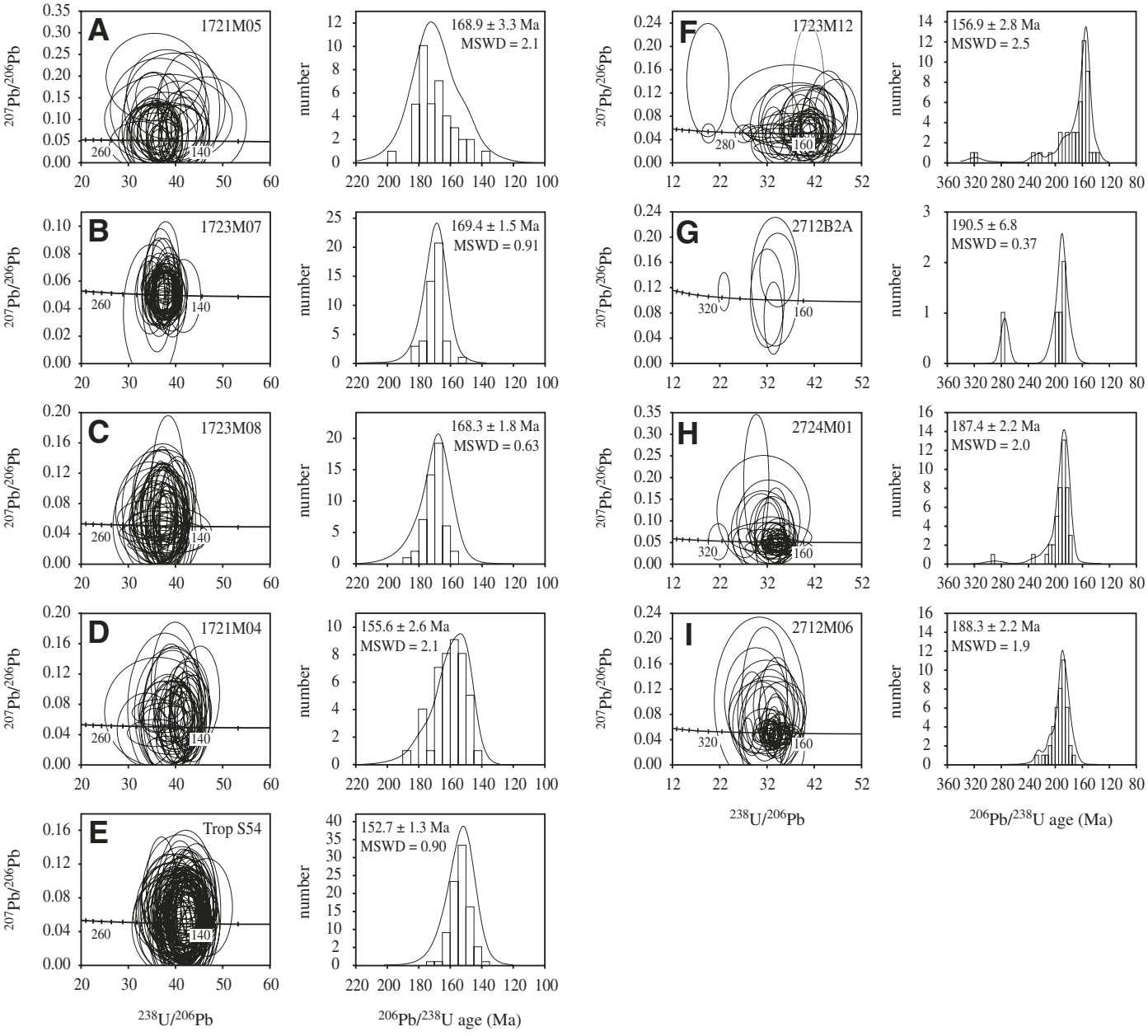

Figure 7. Tera-Wasserburg concordia plots and histograms of laser ablation-inductively coupled plasma-mass spectrometry U-Pb zircon data. Spot analyses of samples 1723M12, 2712B2a, 2724M01, and 2712M06 record evidence for inheritance of Triassic–Carboniferous xenocrystic zircons. The ages within the histogram plots are weighted mean $^{206}Pb/^{238}U$ ages with 2σ errors; 3σ outliers (i.e., the inherited ages) were excluded from the weighted-mean calculations for samples 1723M12, 2712B2A, 2724M01, and 2712M06 to focus the mean on the Jurassic populations. MSWD—mean square of weighted deviates. All error ellipses are 2σ. Ages along concordia are in Ma. All plots were produced using Isoplot 3.0/3.2 (Ludwig, 2003). Analytical details and raw data are in Table DR3 (see footnote 1).

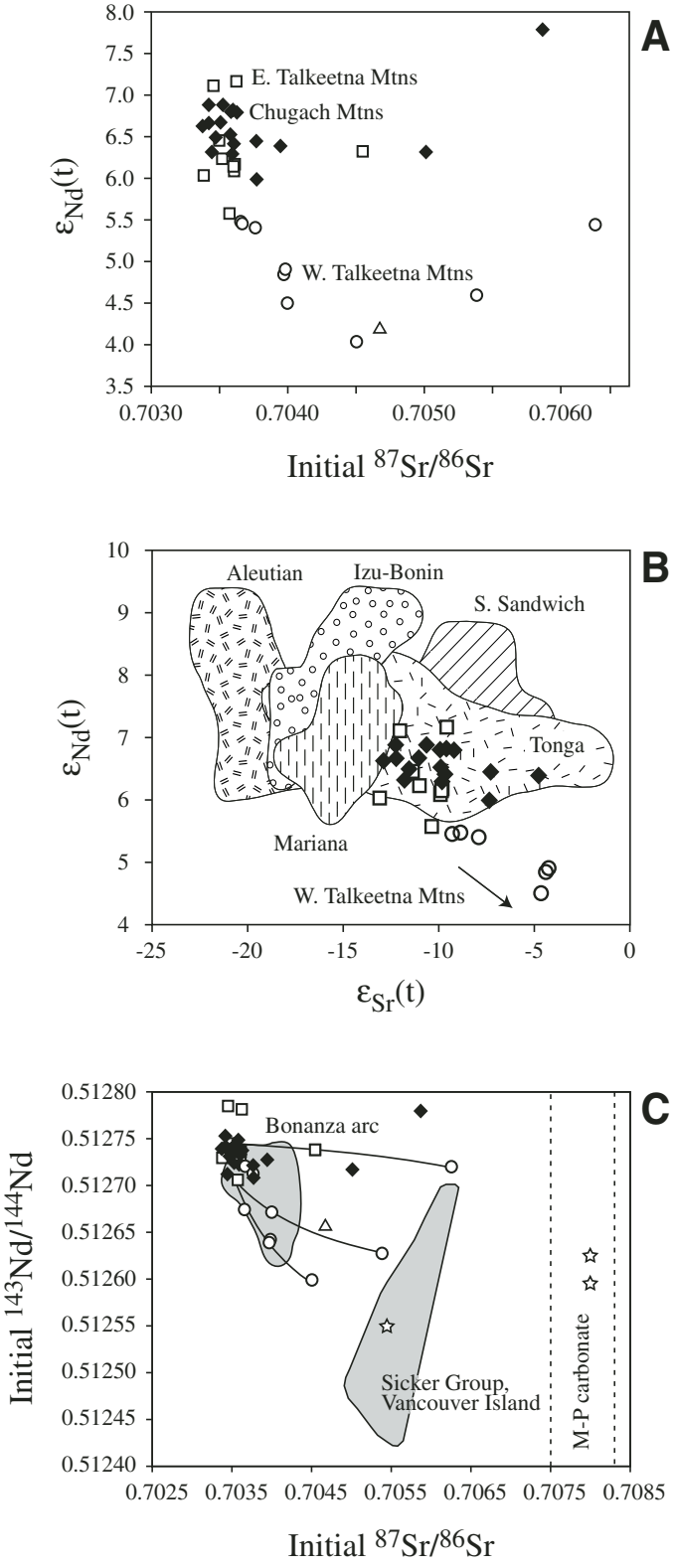

Figure 8. (A) $\varepsilon_{Nd}(t)$ and initial $^{87}Sr/^{86}Sr$ data from the Chugach (diamonds), eastern Talkeetna (squares), and western Talkeetna (circles) Mountains. The single triangular symbol is a sample of metavolcanic wall rock in the western Talkeetna Mountains. The data were corrected to initial values using the ages listed in Table 2. (B) Comparison of age corrected data from the Chugach and Talkeetna Mountains to modern intra-oceanic arcs. Data from the Chugach and eastern Talkeetna Mountains are similar to the Tonga–Kermadec arc, whereas data from the western Talkeetna Mountains have more evolved isotopic values. Modern arc fields are based on data from McCulloch and Perfit (1981), Ewart and Hawkesworth (1987), Woodhead (1989), Pearce et al. (1995), Ewart et al. (1998), Taylor and Nesbitt (1998), and Leat et al. (2003) and were recalculated to be consistent with the standard and normalization values used in this study. The Tonga-Kermadec field excludes data from the northern Tonga islands, which are affected by the Samoan plume and subduction of the Louisville Ridge seamount chain (Ewart et al., 1998). (C) Three calculated mixing lines between arc magma compositions and potential isotopic end members in the Wrangellia terrane (shown as stars). The mixing lines were calculated using the energy-constrained recharge, assimilation, and fractional crystallization (EC-RAFC) program with magma compositions of $^{143}Nd/^{144}Nd$ = 0.512706, 0.512706, 0.512745, $^{87}Sr/^{86}Sr$ = 0.703535, 0.703535, 0.703478, Nd = 5, 5, 15 ppm, Sr = 200, 350, 200 ppm and respective assimilant compositions of $^{143}Nd/^{144}Nd$ = 0.51255, 0.512595, 0.512625, $^{87}Sr/^{86}Sr$ = 0.70545, 0.708, 0.708, Nd = 15, 15, 5 ppm, Sr = 250, 315, 400 ppm. The models do not include magma recharge. Similar results were obtained with a range of parameters. The Bonanza arc and Sicker Group fields are based on data from Samson et al. (1990) and Andrew et al. (1991) corrected to initial values at 175 Ma. Mississippian to Pennsylvanian marine carbonate (M-P carbonate) data are from Burke et al. (1982), Denison et al. (1994), and Veizer et al. (1999).

TABLE 2. Sm-Nd AND Rb-Sr DATA FROM THE CHUGACH AND TALKEETNA MOUNTAINS

Sample	Sm	Nd	$^{147}Sm/^{144}Nd$	$^{143}Nd/^{144}Nd$	$2\sigma^{\dagger}$	$\varepsilon_{Nd}(t)^{\ddagger}$	Rb	Sr	$^{87}Rb/^{86}Sr$	$^{87}Sr/^{86}Sr$	$2\sigma^{\dagger}$	$^{87}Sr/^{86}Sr_{int}{}^{\ddagger}$	$\varepsilon_{Sr}(t)^{\ddagger}$	Age[§] (Ma)
Chugach Mountains														
0716P01	2.5	9.8	0.156	0.512911	5	6.3	4.5	201.8	0.064	0.703764	10	0.703595	–9.8	185.1
0717B03	0.6	3.0	0.124	0.512857	12	6.0	4.8	337.4	0.042	0.703878	15	0.703770	–7.3	184.1
0718P01B	3.1	11.6	0.163	0.512926	5	6.4	14.7	172.6	0.247	0.704245	11	0.703609	–9.7	181.4
0719P05B	2.9	11.4	0.151	0.512928	6	6.8	22.9	172.4	0.385	0.704687	13	0.703629	–9.2	193.3
0719P05B	2.8	11.1	0.153	0.512936	9	6.9	22.8	170.1	0.388	0.704593	12	0.703527	–10.6	193.3
0720G02	4.5	14.2	0.192	0.512965	8	6.5	14.3	241.9	0.172	0.703926	10	0.703472	–11.5	186.1
1709A02	1.0	3.2	0.192	0.512956	30	6.3	1.9	256.5	0.021	0.705073	19	0.705017	10.3	181
1722A11[#]	0.6	1.4	0.260	0.513041	8	6.4	0.0	293.6	0.000	0.703952	18	0.703951	–4.7	185
1723A03[#]	0.4	0.8	0.278	0.513085	11	6.8	0.0	226.3	0.001	0.703589	16	0.703587	–9.9	185
1724M01	3.8	12.9	0.178	0.512967	4	6.9	11.6	235.5	0.143	0.703798	11	0.703423	–12.2	185
1727M04	2.4	7.6	0.191	0.512972	7	6.7	6.7	280.8	0.069	0.703605	12	0.703424	–12.2	185
1728A03[#]	1.1	3.2	0.207	0.512981	25	6.4	9.6	236.9	0.117	0.704082	22	0.703774	–7.3	185
2713M03	0.7	2.1	0.206	0.512989	13	6.6	0.7	344.2	0.006	0.703394	14	0.703379	–12.9	185
2714M02	3.1	10.6	0.179	0.512959	8	6.7	7.1	232.4	0.089	0.703743	13	0.703508	–11.0	186.1
2716M02	1.4	4.2	0.206	0.512973	6	6.3	2.0	338.7	0.017	0.703493	11	0.703445	–11.8	194
2717M01	1.5	5.1	0.180	0.512951	4	6.5	13.5	260.1	0.151	0.703994	12	0.703578	–9.9	194
2717M04	2.1	8.1	0.160	0.512940	11	6.8	12.2	464.5	0.076	0.703810	10	0.703600	–9.6	193.9
2717P06A	4.0	18.5	0.132	0.512952	3	7.8	0.1	23.3	0.015	0.705909	21	0.705867	22.7	200
Eastern Talkeetna Mountains														
1721M01	3.8	14.1	0.165	0.512916	4	6.1	35.4	188.2	0.544	0.704959	12	0.703603	–9.8	175.5
1721M05	3.6	12.1	0.179	0.512903	5	5.6	6.8	349.7	0.056	0.703710	18	0.703574	–10.4	169
1723M01	1.4	5.3	0.157	0.512905	12	6.1	5.3	434.5	0.035	0.703692	11	0.703607	–9.9	168.9
1723M02	2.1	8.8	0.144	0.512896	11	6.2	11.1	353.1	0.091	0.703831	11	0.703613	–9.8	169
1723M04	4.7	17.1	0.165	0.512921	5	6.2	42.8	187.9	0.659	0.705177	11	0.703520	–11.0	176.9
1723M06	1.1	2.9	0.228	0.513037	17	7.1	26.9	129.2	0.602	0.704904	21	0.703456	–12.0	169
1723M07	2.8	9.5	0.177	0.512926	4	6.0	8.8	301.9	0.085	0.703586	13	0.703383	–13.1	169
1723M09	2.8	11.5	0.146	0.512911	11	6.4	57.7	180.9	0.922	0.705775	21	0.703498	–11.4	173.7
4713M01	4.3	16.6	0.155	0.512958	16	7.2	52.6	216.8	0.702	0.705361	18	0.703624	–9.6	174
4718M06	3.9	15.1	0.155	0.512914	14	6.3	37.7	254.8	0.429	0.705608	27	0.704548	3.5	174
Western Talkeetna Mountains														
1721M04	4.1	15.5	0.159	0.512876	10	5.4	12.6	568.3	0.064	0.703904	11	0.703761	–7.9	157
1723M10	3.2	10.0	0.194	0.512914	13	5.4	5.2	117.1	0.128	0.706531	15	0.706252	27.4	153
1723M12	0.9	4.4	0.128	0.512800	10	4.5	13.1	1063.9	0.036	0.704072	11	0.703995	–4.7	153
2712M06	1.5	6.2	0.150	0.512815	13	4.6	4.2	356.8	0.034	0.705474	13	0.705383	15.7	191
2712P05	0.8	2.6	0.187	0.512833	12	4.0	3.9	140.4	0.080	0.704723	15	0.704505	3.2	191
2722M01	3.4	11.9	0.175	0.512862	10	4.9	0.5	260.9	0.006	0.703995	12	0.703979	–4.2	192
2724M01	2.4	8.3	0.178	0.512862	6	4.8	1.0	305.9	0.009	0.703993	12	0.703968	–4.4	192
4716M07	1.8	6.6	0.170	0.512826	20	4.2	32.8	112.0	0.847	0.706515	19	0.704673	5.0	153
4716M09	1.3	5.9	0.128	0.512849	14	5.5	16.6	1014.7	0.047	0.703770	18	0.703667	–9.3	153
4724M03	3.7	14.8	0.150	0.512861	18	5.5	17.6	504.1	0.101	0.703929	16	0.703656	–8.9	190

[†]2σ absolute errors—reported values are in units of 10^{-6}.

[‡]$\varepsilon_{Nd}(t)$ were calculated using present-day bulk-earth values of $^{143}Nd/^{144}Nd = 0.512638$ and $^{147}Sm/^{144}Nd = 0.1967$, and a ^{147}Sm decay constant of 6.54×10^{-12} yr^{-1}. $\varepsilon_{Sr}(t)$ and $^{87}Sr/^{86}Sr_{int}$ were calculated using present-day bulk-earth values of $^{87}Sr/^{86}Sr = 0.7045$ and $^{87}Rb/^{86}Sr = 0.0816$, and an ^{87}Rb decay constant of 1.42×10^{-11} yr^{-1}.

[§]Ages used for calculating the epsilon and initial isotopic values. Values given to 1 decimal place are based on U-Pb zircon ages from the same sample. Values with no decimal are either inferred from field relationships with dated units or determined from complex U-Pb zircon results.

[#]Sm and Nd data are from Greene et al. (2006).

margin of the Jtr pluton gave $\varepsilon_{Nd}(t)$ = 4.2 and $^{87}Sr/^{86}Sr_{int}$ = 0.704673. The anomalous $^{87}Sr/^{86}Sr$ values for samples 2717P06A, 1709A2, and 4718M06 most likely reflect disturbance of the Rb-Sr system, which is sensitive to secondary alteration, or organic interferences during the MC-ICP-MS analyses. The coherence of the rest of the data suggests that both Rb-Sr and Sm-Nd were closed systems in most samples.

DISCUSSION

Magmatic Evolution of the Talkeetna Arc

Our new data from the Chugach Mountains indicate that the main phase of Talkeetna arc magmatism lasted from 202.1 to 181.4 Ma. Two samples from mid-crustal lithologies preserved in the Klanelneechena klippe (Fig. 2) yielded ages from 201.8 to 198.7 Ma and overlap the oldest age from the arc section north of the Border Ranges fault. The restricted range in the initial isotopic ratios [$\varepsilon_{Nd}(t)$ = 6.0–7.8 and $^{87}Sr/^{86}Sr_{int}$ = 0.703379–0.703951] from the Chugach Mountains is similar to modern intra-oceanic arcs and demonstrates the juvenile nature of the arc plutons. The data correlate closely with the range in epsilon values from the central Tonga-Kermadec arc (Fig. 8B), which are interpreted to reflect multicomponent mixing between a variably depleted mantle wedge, a slab-derived fluid, and melt of subducted sediment (Turner et al., 1997; Ewart et al., 1998; Haase et al., 2002). The arc-like isotopic ratios and absence of inherited zircons in the Chugach Mountain plutons suggest that any preexisting basement had little or no impact on the geochemical evolution of the arc in this area.

Data from the Talkeetna Mountains are more complex than the Chugach analyses and define two distinct crustal domains. Plutons from the eastern Talkeetna Mountains (Jgd and Jqd), which intrude northern exposures of the Talkeetna arc volcanic sequence, record crystallization ages between 177.5 and 168.9 Ma and have oceanic-arc-like isotopic ratios [$\varepsilon_{Nd}(t)$ = 5.6–7.2 and $^{87}Sr/^{86}Sr_{int}$ = 0.703383–0.703624; Fig. 8B]. Minor disturbance of U-Pb zircon ages in these units (i.e., Jqd analyses) can be explained by assimilation of adjacent arc plutonic rocks. Conversely, samples from the central and western Talkeetna Mountains (Jtr, Jpmu, and Jgdw) have complex U-Pb zircon data and evolved isotopic signatures [$\varepsilon_{Nd}(t)$ = 4.0–5.5 and $^{87}Sr/^{86}Sr_{int}$ = 0.703656–0.706252; Fig. 8]. The laser-ablation and chemical-abrasion analyses from these samples indicate that the U-Pb systematics reflect incorporation of Carboniferous–Triassic (320–220 Ma) zircons into Jurassic (ca. 190–153 Ma) magmas. The young trondhjemite pluton (152.7 ± 1.3 Ma) in the center of the Talkeetna Mountains marks the boundary between the juvenile arc plutons in the eastern Talkeetna Mountains and isotopically evolved older plutons (ca. 190 Ma) along the western margin of the batholith (Figs. 2 and 9).

The progression of U-Pb ages from the Chugach to Talkeetna Mountains indicates that the Talkeetna arc was active for ~50 m.y. from the Early to Middle Jurassic (Fig. 9). The range of U-Pb ages from the Chugach Mountains suggests repeated intrusion of arc magmas along a single magmatic axis from 202.1 to 181.4 Ma. This was followed by a northward migration (present coordinates) of the arc magmatic axis between 181.4 and 177.5 Ma and intrusion of plutons in the Talkeetna Mountains. New and existing K-Ar and ^{40}Ar-^{39}Ar cooling ages mirror the trend in the U-Pb data: ^{40}Ar-^{39}Ar hornblende cooling ages from the Chugach Mountains range from 189 to 160 Ma (Onstott et al., 1989; Plafker et al., 1989; Hacker et al., 2006a; K-Ar = 194–135 Ma; Winkler et al., 1981; Pavlis, 1982, 1983; Plafker et al., 1989; Burns et al., 1991; Winkler, 1992), whereas ages from the Talkeetna Mountains range from 178 to 145 Ma (Hacker et al., 2006a; K-Ar = 173–154 Ma; Csejtey et al., 1978). Geochemical analyses of Talkeetna Formation volcanic rocks from the Talkeetna Mountains record backarc geochemical signatures consistent with northward subduction of oceanic lithosphere beneath the arc (Clift et al., 2005a). The northward shift in the arc magmatic axis from the Chugach into the Talkeetna Mountains may therefore reflect either shallowing of the subducting slab (Plafker et al., 1989) or tectonic erosion of the forearc (Clift et al., 2005b). The ca. 190–153 Ma plutons with inherited zircon and evolved isotopic signatures in the western Talkeetna Mountains require the interaction of Jurassic magmas with Paleozoic crustal material and are discussed further below.

Interaction with the Wrangellia Terrane

The age of the inherited zircons and the isotopic signatures of plutons from the central and western Talkeetna Mountains are consistent with assimilation of basement lithologies from the adjacent Wrangellia terrane. In southern Alaska, the Wrangellia terrane is composed of the Paleozoic Skolai arc, the extensive Triassic Nikolai flood basalts, and interspersed metasedimentary units (e.g., Barker et al., 1994; Nokleberg et al., 1994). The U-Pb zircon ages from Skolai arc plutons range from 316 to 290 Ma (Beard and Barker, 1989) and pre-Nikolai fossil ages are as old as Early Pennsylvanian (Plafker et al., 1985). The Wrangellia terrane in the Talkeetna Mountains was originally interpreted as a thick section of Pennsylvanian–Early Permian arc volcanic rocks with interspersed metasedimentary bodies (Csejtey et al., 1978); however, more recent analyses suggest that the section consists principally of Nikolai basalt, Paleozoic–Triassic metasedimentary rocks, and undated (Triassic or older) microgabbro (Schmidt et al., 2003). Metasedimentary rocks include siliceous metasiltstone, phyllite, calc-silicate–bearing metatuff, and metalimestone (Csejtey et al., 1978; Schmidt et al., 2003). There are no isotopic data from the pre-Nikolai units in southern Alaska, but correlative Devonian arc lithologies and associated Pennsylvanian–Devonian metasedimentary rocks from the Wrangellia basement on Vancouver Island, British Columbia, have low positive $\varepsilon_{Nd}(t)$ and a broad range of $^{87}Sr/^{86}Sr_{int}$ (Fig. 8C; note that the Sr compositions from the Wrangellian basement lithologies are suspect and may be affected by secondary alteration or interaction with seawater; Samson et al., 1990; Andrew et al., 1991). In addition, global Mississippian–Pennsylvanian marine carbonate sequences have elevated $^{87}Sr/^{86}Sr$ of 0.70755–0.70830 (Burke et al., 1982; Denison et al., 1994; Veizer et al., 1999).

To model the assimilation of older Wrangellian crust into arc magma compositions we used the energy-constrained recharge, assimilation, and fractional crystallization (EC-RAFC) formulation developed by Spera and Bohrson (2001, 2002; Bohrson and Spera, 2001, 2003). The EC-RAFC program uses energy-constrained thermodynamic calculations to model the geochemical evolution of a cooling magma body and its interaction with the surrounding country rock. Figure 8C shows three examples of EC-RAFC mixing lines between arc magma compositions and potential end-member compositions from the Wrangellia terrane. The mixing lines track the isotopic evolution of magmas from estimated liquidus temperatures (1125 °C) to equilibration with the surrounding country rock (846 °C) and recreate the isotopic compositions of plutonic rocks from the western Talkeetna Mountains. The outcome of the mixing calculations depends on the concentration and isotopic composition of Nd and Sr in the mixing end members, and as a result there are multiple combinations of host and assimilant compositions that can explain each datum from the western Talkeetna Mountains. However, all the mixing models require a range of assimilant compositions, variable degrees of crustal assimilation, and/or variable Nd and Sr concentrations in the host magmas to account for the total variations within and among the different plutons. These conditions are consistent with the diverse compositions of arc magmas and the range of implied isotopic values for potential assimilants in the Wrangellia section. The Bonanza arc field

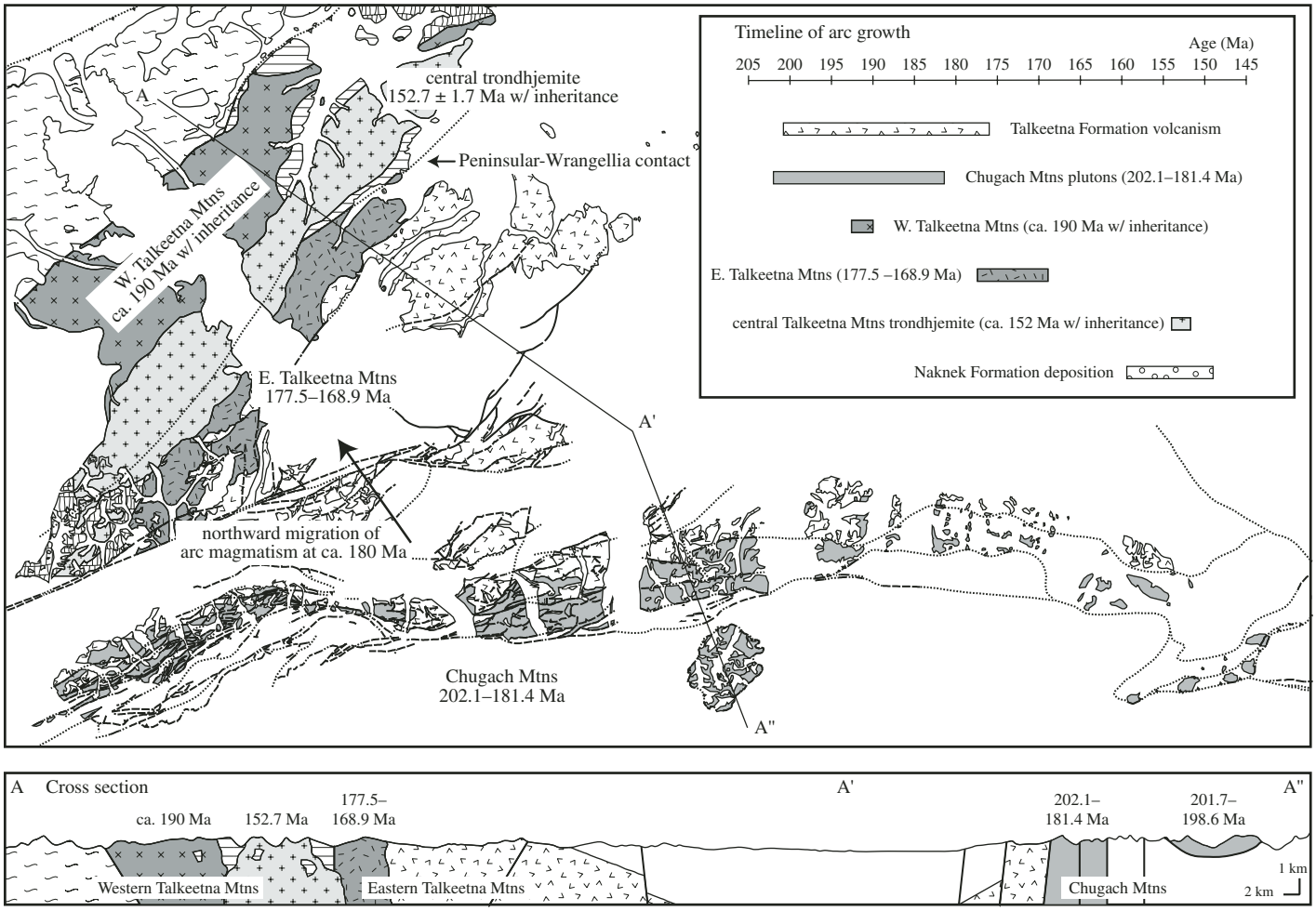

Figure 9. Summary of the tectonic development of the Talkeetna arc and a northwest cross section through the Talkeetna and Chugach Mountains. The time span of Talkeetna arc volcanism is based on the fossil ages from the Talkeetna Mountains and the Alaska Peninsula (Grantz et al., 1963; Imlay, 1984) and the depositional history of the Naknek Formation is from Trop et al. (2005). The map references, latitude, longitude, and scale are given in Figure 2.

in Figure 8C shows the range in isotopic ratios from Jurassic plutonic and volcanic lithologies on Vancouver Island. The Bonanza arc intruded a thick section of Wrangellia crust—including the Paleozoic Sicker group and Triassic Karmutsen flood basalts (Isachsen, 1987; DeBari et al., 1999)—and the range in isotopic values may represent an analogue for the assimilation of older Wrangellian crust into arc plutons in the western Talkeetna Mountains.

The Peninsular-Wrangellia contact in the Talkeetna Mountains was originally mapped as a pre-Cretaceous thrust fault that places Jurassic plutonic rocks (Jpmu and Jgdw) of the Peninsular terrane over the metavolcanic rocks (PzTrm) of the Wrangellia terrane (Fig. 2; Csejtey et al., 1978). However, the evidence for assimilation of Paleozoic wall rocks into Jurassic plutons south of the fault suggests that Wrangellia crust extends into the central Talkeetna Mountains. Specifically, the isotopic data suggest that the terrane margin parallels the trend of the Jtr pluton along the dashed line in Figure 9. This proposed boundary is consistent with a distinct geomagnetic and gravity gradient that Glen et al. (2007) independently interpreted as the Peninsular-Wrangellia contact. Early Jurassic plutons north of the boundary (Jpmu and Jgdw; Fig. 2) may represent either early Talkeetna arc plutonism or a previously unidentified component of Wrangellia crust. The Jtr pluton intrudes the refined terrane boundary and requires that the Peninsular and Wrangellia terranes were stitched into a single tectonic block by ca. 153 Ma.

Termination of Arc Magmatism

The end of Talkeetna arc magmatism was coeval with regional shortening and uplift in the Peninsular and Wrangellia terranes (Trop et al., 2005). Fossil successions from the Talkeetna Formation volcanic rocks and overlying sedimentary units in the Talkeetna Mountains and on the Alaska Peninsula suggest that final arc volcanism occurred between the late Toarcian and middle Bajocian (180.1 ± 4.0–169.2 ± 4.0 Ma; Grantz et al., 1963; Imlay, 1984; Gradstein et al., 1995). This was followed by the cessation of arc plutonism ca. 153 Ma, recorded by intrusion of the trondhjemite pluton in the central Talkeetna Mountains. Trop et al. (2005) presented sedimentary analyses from the Naknek Formation in the eastern Talkeetna Mountains that document active unroofing of the Talkeetna arc volcanic and plutonic lithologies from the early Oxfordian to early Tithonian (159.4–149.0 Ma; Gradstein et al., 1995) and coeval shortening of the sedimentary section. This uplift was synchronous with contractional structures and unroofing sequences on the inboard (continental) side of the Peninsular

and Wrangellia terranes in the Kahiltna Basin (Ridgway et al., 2002) and Wrangell Mountains Basin (Trop et al., 2002, 2005).

Tectonic Implications

The interaction between the evolution of Talkeetna arc magmatism and large-scale deformation in southern Alaska is consistent with at least two tectonic models (Fig. 10).

1. The near-synchronous termination of Talkeetna arc magmatism and corresponding regional uplift may reflect the amalgamation of the Talkeetna arc and the Wrangellia terrane prior to final accretion onto the continental margin (Fig. 10B). If so, the Peninsular–Wrangellia contact defined by the isotopic data represents a suture between the two terranes. As discussed above, the central trondhjemite intruded along the contact and requires the amalgamation of the terranes by ca. 153 Ma. The isotopically evolved ca. 190 Ma plutons in the western Talkeetna Mountains must then preserve evidence for Early Jurassic arc magmatism within Wrangellia and could represent a northern extension of the Bonanza arc on Vancouver Island. This interpretation is consistent with the distinct break in U-Pb systematics and initial isotopic ratios between the eastern and western Talkeetna Mountains. The modern Japan–Izu Bonin collision in the western Pacific provides a modern analogue for this type of arc-arc collision.

2. Alternatively, the observed temporal evolution may reflect the final accretion of a combined Wrangellia-Peninsular terrane onto the North American margin (e.g., Ridgway et al., 2002; Trop et al., 2002; Fig. 10C). Plafker et al. (1989) and others argued that similar Permian carbonates, Triassic basalts, and Jurassic arc assemblages (i.e., the Talkeetna and Bonanza arc) in the Peninsular and Wrangellia terranes may reflect either pre-Jurassic juxtaposition of the two terranes or formation as a single tectonic block (Nokleberg et al., 1994). Under these circumstances, the Talkeetna arc may have formed as a trailing arc to the larger Wrangellia terrane. The ca. 190 Ma plutons in the eastern Talkeetna Mountains may reflect early arc-related magmatism that intruded through the Wrangellia plateau, while the main volume of arc magmas intruded thinner oceanic crust.

CONCLUSIONS

New high-precision U-Pb zircon and radiogenic isotope data from the accreted Talkeetna arc document the temporal and geochemical evolution of the arc over ~50 m.y. from the Early to Middle Jurassic. Plutonic lithologies in the main arc section in the Chugach Mountains were emplaced from 202.1 to 181.4 Ma and have intra-oceanic arc–like isotopic ratios [$\varepsilon_{Nd}(t)$ = 6.0–7.8 and $^{87}Sr/^{86}Sr_{int}$ = 0.703379–0.703951]. The arc magmatic axis subsequently shifted northward between 181.4 and 177.5 Ma, leading to the generation of the large plutonic suite in the Talkeetna Mountains. Data from the Talkeetna Mountains define two distinct crustal domains. Plutons from the eastern Talkeetna Mountains have intra-oceanic arc–like isotopic ratios and record U-Pb zircon crystallization ages of 177.5–168.9 Ma. In contrast, samples from the western Talkeetna Mountains are characterized by more evolved isotopic ratios and evidence for inheritance of Carboniferous–Triassic zircons. The young (152.7 ± 1.7 Ma) trondhjemite pluton from the central Talkeetna Mountains marks the boundary between the juvenile plutons from the eastern Talkeetna Mountains and isotopically more evolved ca. 190 Ma intrusions along the western margin of the batholith. The evolved Early Jurassic plutonism may represent either a northern extension of the early Talkeetna arc magmatism or a previously unidentified component of Wrangellia crust. The cessation of Talkeetna arc magmatism was coincident with regional shortening, uplift, and the erosion of arc plutons and most likely reflects the amalgamation of the Peninsular and Wrangellia terranes or the accretion of a composite terrane onto continental North America. The intra-oceanic arc–like isotopic signatures and dearth of inherited zircon from the Chugach and eastern Talkeetna Mountains indicate that little or no preexisting crustal material was involved in the generation of the main volume of Talkeetna arc magmas. These data confirm that the Talkeetna arc is an ideal place to study intra-oceanic arc magmatic processes at depth.

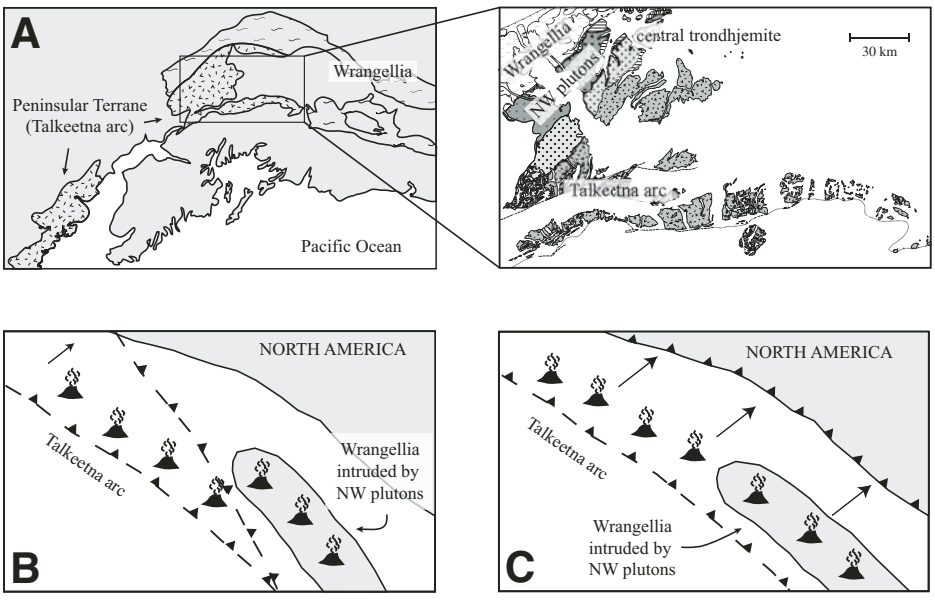

Figure 10. Tectonic models for the Talkeetna arc. (A) Current map configuration of the Wrangellia and Peninsular terranes. (B) Two terrane model: the Talkeetna arc formed as an independent intra-oceanic arc between 202.1 and 168.9 Ma. Subsequent accretion onto Wrangellia ca. 153 Ma led to the termination of arc magmatism and exhumation and erosion of arc plutonic rocks. This tectonic model is analogous to the modern collision between the Izu-Bonin arc and Japan. (C) Single terrane model: the Talkeetna arc formed as a trailing arc to the larger Wrangellia terrane. The termination of arc magmatism may then reflect accretion of the composite terrane onto continental North America. See the text for detailed discussions of the two models. Latitude and longitude for A are shown in Figures 1 and 2.

APPENDIX

U-Pb Error Analysis

All errors for the multigrain CA-TIMS analyses were calculated following Mattinson (1987). Uncertainties on individual digestion steps are reported and plotted at the 2σ level and were calculated as:

$$2\sigma_{207/206} = \{[2*SE(M)_{207/206}]^2 + [0.03\%]^2 + [2\sigma_{common}]^2\}^{1/2},$$

$$2\sigma_{206/238} = \{[2*SE(M)_{205/206}]^2 + [2*SE(M)_{238/235}]^2 + [2\sigma_{common}]^2 + [0.2\%]^2\}^{1/2},$$

$$2\sigma_{207/235} = [(2\sigma_{206/238})^2 + (2\sigma_{207/206})^2]^{1/2},$$

where SE(M) is the standard error of the mean of the measured ratio, 0.03% is the uncertainty in the $^{207}Pb/^{206}Pb$ fractionation correction, $2\sigma_{common}$ is the error associated with the common-Pb correction, and 0.2% is the observed $^{206}Pb/^{238}U$ error in repeat analyses of well-characterized natural samples. Each analysis was corrected for common Pb based on the measured $^{206}Pb/^{204}Pb$. We assumed a Jurassic (200 Ma) common-Pb value (Stacey and Kramers, 1975) for the lowest temperature clean-up steps (A) and estimated blank ratios for the higher temperature digestion steps (B through residue). Propagated common-Pb errors include the precision of the $^{206}Pb/^{204}Pb$ measurement and conservative absolute errors of ±0.2 and ±0.5 for the assumed $^{207}Pb/^{204}Pb_{common}$ and $^{206}Pb/^{204}Pb_{common}$. The replicate error (0.2%) in the $^{206}Pb/^{238}U$ analyses incorporates the uncertainty in the U and Pb fractionation corrections. Final sample ages and propagated errors were calculated as the weighted mean of concordant high-temperature digestion steps using Isoplot 3.0/3.2 (Ludwig, 2003). All the weighted mean errors are reported at the 95% confidence level. Analyses with a probability of fit <15% include a Student's t factor in the calculated uncertainties. Errors on the single-grain analyses carried out at MIT follow Ludwig (1980).

In addition to the random errors associated with individual analyses, the tracer calibration and U decay constant uncertainties introduce systematic errors in the calculated ages. Interlaboratory comparison of absolute ages for the Temora and R33 zircon standards indicate that our spike calibration is accurate to ~0.1%–0.2%. Counting statistics during the measurement of the U half-lives yield minimum 2σ uncertainties on the ^{238}U and ^{235}U decay constants of ±0.107% and ±0.136%, respectively (Jaffey et al., 1971; Mattinson, 1987). The resulting 2σ uncertainties on concordia are shown as a gray band in Figures 4–6. Two recent assessments of the ^{238}U and ^{235}U decay constants using high-precision U-Pb zircon data suggest that one or both of the decay constants require slight revision within the analytical errors of the original counting experiments (Mattinson, 2000; Schoene et al., 2006). Assuming the better determined ^{238}U decay constant is accurate, both studies calculate a new ^{235}U decay constant of $\sim 9.857 \times 10^{-10}$ yr^{-1} (Mattinson, 2000; Schoene et al., 2006), resulting in an upward shift in the position of concordia on a Tera-Wasserburg diagram. The revised concordia is shown as a dashed line in Figures 4–6 and permits more accurate assessment of the concordance or slight discordance of high-precision U-Pb data. The U-Pb ages reported in this paper are based on weighted mean $^{206}Pb/^{238}U$ ages of concordant or near concordant analyses. Reported errors on weighted mean ages in the text, figures, and tables were calculated as the quadratic sum of the weighted mean error (calculated from the random analytical errors) and the systematic error in the tracer calibration (0.15%). Errors on individual step or grain analyses (Tables DR1 and DR2; see footnote 1) do not include the systematic errors.

Zircon Laser Ablation and Whole-Rock Radiogenic Isotope Analytical Procedures

Zircons for LA-ICP-MS dating were mounted in an epoxy grain mount, polished to expose grain cores, and imaged by cathodoluminescence (CL) prior to analysis. All grains were analyzed during a three-day analytical session using the New Wave (Merchantek) 193 nm ArF laser and GV Isoprobe multicollector (MC)-ICP-MS at the University of Arizona. Individual spots were ablated for 20 s at 32 mJ with a repetition rate of 8 Hz and a 50 μm spot size. Each analysis generated an ~15-μm-deep pit. Ablated material was transported to the ICP in a mixed Ar-He carrier gas and ionized in a dry plasma. The He carrier gas contains negligible ^{204}Hg and we corrected for any interference on mass 204 as part of the background measurement. Mass 204 was measured on an ion counter and masses 206, 207, 208, 232, and 238 were measured on Faraday cups in static collection mode. Laser-induced fractionation generally varied with pit depth/analysis time, and we used a linear regression of isotopic ratios (e.g., $^{206}Pb/^{238}U$, $^{207}Pb/^{206}Pb$) versus time, excluding 3σ outliers, to project ratios to a zero pit depth. For samples with no statistically significant slope we used the weighted average of the isotopic ratios, excluding outliers, as the zero pit depth ratio. Each unknown was normalized to an in-house Jurassic (183.33 ± 0.11 Ma) zircon standard and the R33 (419.96 ± 0.15 Ma; Mattinson, 2005b) zircon standard, which were analyzed every fourth and eighth spot, respectively. The preferred 419.96 Ma age for the R33 standard is based on recent CA-TIMS analyses (Mattinson, 2005a, 2005b) and is ~0.16% older than the Black et al. (2004) age of 419.26 ± 0.39 Ma. The R33 standards used in the laser analyses were pretreated using the chemical abrasion technique to remove zones of potential Pb loss (Mattinson, 2005a). The raw data were reduced using an Excel macro written by Gehrels and Hacker. For a complete discussion of the LA-ICP-MS parameters and data regression techniques, refer to Hacker et al. (2006b).

Whole-rock samples for isotopic analyses were prepared in the clean laboratory facilities at Boston University. Prior to analysis, samples were hand crushed to 1–2 cm pieces and then powdered in an alumina shatter box. Samples were spiked with ^{149}Sm-^{150}Nd and ^{87}Rb-^{84}Sr tracers and dissolved in Parr bombs using a mixture of 50% HF and 8 N HNO_3. Initial digestions were done in open containers on a hot plate at 90–120 °C (3 ml HNO_3 to 1 ml HF) and final digestions were achieved in an oven at 220 °C for 72 h (3 ml HF to 1 ml HNO_3). Care was taken to ensure complete digestion of refractory minerals such as zircon. Following digestion, solutions were transported to Woods Hole Oceanographic Institute (WHOI) for elemental separation and analysis. Rb, Sr, and the light (L) REEs were separated using cation-exchange column chemistry (following Hart and Brooks, 1977) and Sm and Nd were separated from the LREE aliquot using Di(2-ethylhexyl) orthophosphoric acid (HDEHP) treated columns (following Richard et al., 1976). Isotopic ratios were measured on the ThermoFinnigan Neptune MC-ICP-MS (Nd and Sr) and the ThermoFinnigan Element2 ICP-MS (Sm and Rb). Ratios were corrected to a La Jolla Nd standard value of $^{143}Nd/^{144}Nd = 0.511847$ and an NBS 987 Sr standard value of $^{87}Sr/^{86}Sr = 0.71024$. Data are normalized to $^{146}Nd/^{144}Nd = 0.7219$ and $^{86}Sr/^{88}Sr = 0.1194$. Analytical errors were calculated following Brueckner et al. (2002). For all data, initial isotopic ratios were calculated using our U-Pb zircon ages or the field relationships of samples to dated units.

ACKNOWLEDGMENTS

We thank our collaborators Luc Mehl, Terry Pavlis, Karen Hanghoj, Jeff Trop, Andrew Greene, Mike Johnsen, Sue DeBari, Greg Hirth, Jeff Amato, Peter Clift, Mark Behn, and Amy Draut for helpful discussions and field support in Alaska. Dave Pearson, Karen Vasko, Gabe Rotberg, and Michelle Garde assisted with mineral separations for the U-Pb zircon analyses. Bill McClelland, Sarah Roeske, and G. Lang Farmer provided detailed and useful reviews of the original manuscript. This research was supported by National Science Foundation grant EAR-9910899.

REFERENCES CITED

Andrew, A., Armstrong, R.L., and Runkle, D., 1991, Neodymium-strontium-lead isotopic study of Vancouver Island igneous rocks: Canadian Journal of Earth Sciences, v. 28, p. 1744–1752.

Bard, J.P., 1983, Metamorphism of an obducted island arc: Example of the Kohistan sequence (Pakistan) in the Himalayan collided range: Earth and Planetary Science Letters, v. 65, p. 133–144, doi: 10.1016/0012-821X(83)90195-4.

Barker, F., Aleinikoff, J.N., Box, S., Evans, B.W., Gehrels, G., Hill, M.D., Irving, A.J., Kelley, J.S., Leeman, W.P., Lull, J.S., Nockleberg, W.J., Pallister, J.S., Patrick, B.E., Plafker, G., and Rubin, C.M., 1994, Some accreted volcanic rocks of Alaska and their elemental abundances, *in* Plafker, G., and Berg, H.C., eds., The geology of Alaska: Boulder, Colorado, Geological Society of America, Geology of North America, v. G-1, p. 555–587.

Beard, J.S., and Barker, F., 1989, Petrology and tectonic significance of gabbros, tonalites, shoshonites, and anorthosites in a ;ate Paleozoic arc-root complex in the Wrangellia terrane, southern Alaska: Journal of Geology, v. 97, p. 667–683.

Black, L.P., Kamo, S.L., Allen, C.M., Davis, D.W., Aleinikoff, J.N., Valley, J.W., Mundil, R., Campbell, I.H., Korsch, R.J., Williams, I.S., and Foudoulis, C., 2004, Improved $^{206}Pb/^{238}U$ microprobe geochronology by the monitoring of a trace-element-related matrix effect; SHRIMP, ID–TIMS, ELA–ICP–MS and oxygen isotope documentation for a series of zircon standards: Chemical Geology, v. 205, p. 115–140, doi: 10.1016/j.chemgeo.2004.01.003.

Bohrson, W.A., and Spera, F.J., 2001, Energy-constrained open-system magmatic processes IV: Application of energy-constrained assimilation-fractional crystallization (EC-AFC) model to magmatic systems: Journal of Petrology, v. 42, p. 1019–1041, doi: 10.1093/petrology/42.5.1019.

Bohrson, W.A., and Spera, F.J., 2003, Energy-constrained open-system magmatic processes II: Geochemical, thermal and mass consequences of energy-constrained recharge, assimilation and fractional crystallization (EC-RAFC): Geochemistry, Geophysics, Geosystems, v. 4, doi: 10.1029/2002GC000316.

Bond, G.C., 1973, A late Paleozoic volcanic arc in the eastern Alaska Range, Alaska: Journal of Geology, v. 81, p. 557–575.

Brueckner, H.K., Carswell, D.A., and Griffin, W.L., 2002, Paleozoic diamonds within Precambrian peridotite lens in UHP gneisses of the Norwegian Caledonides: Earth and Planetary Science Letters, v. 203, p. 805–816, doi: 10.1016/S0012-821X(02)00919-6.

Burke, W.H., Denison, R.E., Hetherington, E.A., Koepnick, R.B., Nelson, H.F., and Otto, J.B., 1982, Variation of seawater $^{87}Sr/^{86}Sr$ throughout Phanerozoic time: Geology, v. 10, p. 516–519, doi: 10.1130/0091-7613(1982)10<516:VOSSTP>2.0.CO;2.

Burns, L.E., 1985, The Border Ranges ultramafic and mafic complex, south-central Alaska: cumulate fractionates of island arc volcanics: Canadian Journal of Earth Sciences, v. 22, p. 1020–1038.

Burns, L.E., Pessel, G.H., Little, T.A., Pavlis, T.L., Newberry, R.J., Winkler, G.R., and Decker, J., 1991, Geology of the northern Chugach Mountains, south-central Alaska: Alaska Division of Geological and Geophysical Surveys Professional Report 94, 63 p.

Clift, P.D., Draut, A.E., Kelemen, P.B., Blusztajn, J., and Greene, A., 2005a, Stratigraphic and geochemical evolution of an oceanic arc upper crustal section: The Jurassic Talkeetna Volcanic Formation, south-central Alaska: Geological Society of America Bulletin, v. 117, p. 902–925, doi: 10.1130/B25638.1.

Clift, P.D., Pavlis, T., DeBari, S.M., Draut, A.E., Rioux, M., and Kelemen, P., 2005b, Subduction erosion of the Jurassic Talkeetna-Bonanza arc and the Mesozoic accretionary tectonics of western North America: Geology, v. 33, p. 881–884, doi: 10.1130/G21822.1.

Csejtey, B., Jr., Nelson, W.H., Jones, D.L., Silberling, N.J., Dean, R.M., Morris, M.S., Lanphere, M.A., Smith, J.G., and Silberling, M.L., 1978, Reconnaissance geologic map and geochronology, Talkeetna Mountains

quadrangle, northern part of Anchorage quadrangle, and southwest corner of Healy quadrangle, Alaska: U.S. Geological Survey Open-File Report 78–558A, 62 p., scale 1:250,000.

DeBari, S.M., and Coleman, R.G., 1989, Examination of the deep levels of an island arc: Evidence from the Tonsina ultramafic-mafic assemblage, Tonsina, Alaska: Journal of Geophysical Research, v. 94, p. 4373–4391.

DeBari, S.M., and Sleep, N.H., 1991, High-Mg, low-Al bulk composition of the Talkeetna island arc, Alaska: Implications for primary magmas and the nature of the crust: Geological Society of America Bulletin, v. 103, p. 37–47, doi: 10.1130/0016-7606(1991)103<0037:HMLABC>2.3.CO;2.

DeBari, S.M., Anderson, R.G., and Mortensen, J.K., 1999, Correlation among lower to upper crustal components in an island: The Jurassic Bonanza arc, Vancouver Island, Canada: Canadian Journal of Earth Sciences, v. 36, p. 1371–1413, doi: 10.1139/cjes-36-8-1371.

Denison, R.E., Koepnick, R.B., Burke, W.H., Hetherington, E.A., and Fletcher, A., 1994, Construction of the Mississippian, Pennsylvanian and Permian seawater $^{87}Sr/^{86}Sr$ curve: Chemical Geology, v. 112, p. 145–167, doi: 10.1016/0009-2541(94)90111-2.

Ewart, A., and Hawkesworth, C.J., 1987, The Pleistocene–recent Tonga-Kermadec arc lavas: Interpretation of new isotopic and rare earth data in terms of a depleted mantle source model: Journal of Petrology, v. 28, p. 495–530.

Ewart, A., Collerson, K.D., Regelous, M., Wendt, J.I., and Niu, Y., 1998, Geochemical evolution within the Tonga–Kermadec–Lau arc–back-arc systems: The role of varying mantle wedge composition in space and time: Journal of Petrology, v. 39, p. 331–368, doi: 10.1093/petrology/39.3.331.

Gehrels, G.E., 2001, Geology of the Chatham Sound region, southeast Alaska and coastal British Columbia: Canadian Journal of Earth Sciences, v. 38, p. 1579–1599, doi: 10.1139/cjes-38-11-1579.

Glen, J.M.G., Schmidt, J.M., and Morin, R., 2007, Gravity and magnetic character of south-central Alaska: Constraints on geological and tectonic interpretations, and implications for mineral exploration, *in* Ridgway, K.D., et al., eds., Tectonic growth of a collisional continental margin: Crustal evolution of southern Alaska: Geological Society of America Special Paper 431 (in press).

Gradstein, F.M., Agterberg, F.P., Ogg, J.G., Hardenbol, J., van Veen, P., Thierry, J., and Huang, Z., 1995, A Triassic, Jurassic and Cretaceous time scale, *in* Berggren, W.A., et al., eds., Geochronology, time scales and stratigraphic correlation: SEPM (Society for Sedimentary Geology) Special Publication 54, p. 95–125.

Grantz, A., Thomas, H., Stern, T.W., and Sheffey, N.B., 1963, Potassium-argon and lead-alpha ages for stratigraphically bracketed plutonic rocks in the Talkeetna Mountains, Alaska: U.S. Geological Survey Professional Paper 475-B, p. B56–B59.

Greene, A.R., DeBari, S.M., Kelemen, P.B., Blusztajn, J., and Clift, P.D., 2006, A detailed geochemical study of island arc crust: The Talkeetna arc section, south-central Alaska: Journal of Petrology, v. 47, p. 1051–1093. doi: 10.1093/petrology/eg1002.

Hacker, B.R., Mehl, L., Kelemen, P.B., Rioux, M., and Greene, A., 2005, Reconstructing the Jurassic Talkeetna intra-oceanic arc of Alaska using thermobarometry: Eos (Transactions, American Geophysical Union), v. 86, V51D-1521.

Hacker, B.R., Kelemen, P.B., Rioux, M., McWilliams, M.O., Gans, P.B., and Reiners, P., 2006a, Cooling history of the Talkeetna intra-oceanic arc of Alaska: $^{40}Ar/^{39}Ar$ and U-Th/He dating, *in* Genesis and evolution of the Jurassic Talkeetna Arc of south-central Alaska: Geological Society of America Penrose Conference, Arc Genesis and Crustal Evolution, Valdez, Alaska, 9–15 July 2006, Guidebook, p. 41–45.

Hacker, B.R., Wallis, S.R., Ratschbacher, L., Grove, M., and Gehrels, G., 2006b, High-temperature geochronology constraints on the tectonic history and architecture of the ultrahigh-pressure Dabie Sulu orogen: Tectonics, v. 25, TC5006, doi: 10.1029/2005TC001937.

Hart, S.R., and Brooks, C., 1977, Geochemistry and evolution of early Precambrian mantle: Contributions to Mineralogy and Petrology, v. 61, p. 109–128, doi: 10.1007/BF00374362.

Haase, K.M., Worthington, T.J., Stoffers, P., Garbe-Schönberg, D., and Wright, I., 2002, Mantle dynamics, element recycling, and magma genesis beneath the Kermadec arc–Havre trough: Geochemistry, Geophysics: Geosystems, v. 3, doi: 10.1029/2002GC000335.

Hudson, T., 1979, Mesozoic plutonic belts of southern Alaska: Geology, v. 7, p. 230–234, doi: 10.1130/0091-7613(1979)7<230:MPBOSA>2.0.CO;2.

Hudson, T.L., Arth, J.G., Winkler, G.W., and Stern, T.W., 1985, Jurassic plutonism along the Gulf of Alaska: Geological Society of America Abstract with Programs, v. 17, no. 6, p. 362.

Imlay, R.W., 1984, Early and Middle Bajocian (Middle Jurassic) Ammonites from southern Alaska: U.S. Geological Survey Professional Paper 1322, 38 p.

Isachsen, C.E., 1987, Geology, geochemistry, and cooling history of the West Coast Crystalline Complex and related rocks, Meares Island and vicinity, Vancouver Island, British Columbia: Canadian Journal of Earth Sciences, v. 24, p. 2047–2064.

Jaffey, A.H., Flynn, K.F., Glendenin, L.E., Bentley, W.C., and Essling, A.M., 1971, Precision measurement of half-lives and specific activities of ^{235}U and ^{238}U: Physical Review Series C, v. 4, p. 1889–1906, doi: 10.1103/PhysRevC.4.1889.

Jones, D.L., and Silberling, N.J., 1979, Mesozoic stratigraphy—The key to tectonic analysis of southern and central Alaska: U.S. Geological Survey Open-File Report 79–1200, 37 p.

Kelemen, P.B., Hangøj, K., and Greene, A.R., 2003a, One view of the geochemistry of subduction-related magmatic arcs, with an emphasis on primitive andesite and lower crust, *in* Rudnick, R. et al., eds., Treaties on geochemistry 3: New York, Elsevier, p. 593–659.

Kelemen, P.B., Rilling, J.L., Parmentier, E.M., Mehl, L., and Hacker, B.R., 2003b, Thermal structure due to solid-state flow in the mantle wedge beneath arcs, *in* Eiler, J., ed., Inside the subduction factory: American Geophysical Union Geophysical Monograph 138, p. 293–311.

Khan, M.A., Stern, R.J., Gribble, R.F., and Windley, B.F., 1997, Geochemical and isotopic constraints on subduction polarity, magma sources, and paleogeography of the Kohistan intra-oceanic arc, northern Pakistan Himalaya: Geological Society [London] Journal, v. 154, p. 935–946.

Krogh, T.E., 1973, A low-contamination method for hydrothermal decomposition of zircon and extraction of U and Pb for isotopic age determinations: Geochimica et Cosmochimica Acta, v. 37, p. 485–494, doi: 10.1016/0016-7037(73)90213-5.

Leat, P.T., Smellie, J.L., Millar, I.L., and Larter, R.D., 2003, Magmatism in the south Sandwich arc, *in* Larter, L.D., and Leat, P.T., eds., Intra-oceanic subduction systems: Tectonic and magmatic processes: Geological Society [London] Special Publication 219, p. 239–254.

Le Maitre, R.W., Streckeisen, A., Zanettin, B., Le Bas, M.J., Bonin, B., Bateman, P., Bellieni, G., Dudek, A., Efremova, S., Keller, J., Lameyre, J., Sabine, P.A., Schmid, R., Sørensen, H., and Woolley, A.R., 2002, Igneous rocks: A classification and glossary of terms (second edition): Cambridge, Cambridge University Press, 236 p.

Ludwig, K.R., 1980, Calculation of uncertainties of U-Pb isotope data: Earth and Planetary Science Letters, v. 46, p. 212–220, doi: 10.1016/0012-821X(80)90007-2.

Ludwig, K.R., 2003, User's manual for Isoplot 3.00: A geochronological toolkit for Microsoft Excel: Berkeley Geochronology Center Special Publication 4, 70 p.

Mattinson, J.M., 1987, U-Pb ages of zircons: A basic examination of error propagation: Chemical Geology, v. 66, p. 151–162.

Mattinson, J.M., 1994, A study of complex discordance in zircons using step-wise dissolution techniques: Contributions to Mineralogy and Petrology, v. 116, p. 117–129, doi: 10.1007/BF00310694.

Mattinson, J.M., 2000, Revising the "gold standard"—The uranium decay constants of Jaffey et al., 1971: Eos (Transactions, American Geophysical Union), v. 81, p. V61A–02.

Mattinson, J.M., 2003, CA (chemical abrasion)–TIMS: High resolution U-Pb zircon geochronology combining high temperature annealing of radiation damage and multi-step partial dissolution analysis: Eos (Transactions, American Geophysical Union), v. 84, p. V22E–06.

Mattinson, J.M., 2005a, Zircon U-Pb chemical abrasion ("CA-TIMS") method: Combined annealing and multi-step partial dissolution analysis for improved precision and accuracy of zircon ages: Chemical Geology, v. 220, p. 47–66, doi: 10.1016/j.chemgeo.2005.03.011.

Mattinson, J.M., 2005b, U-Pb inter-laboratory calibrations using zircon samples: Application of the new CA-TIMS technique: Geochimica et Cosmochimica Acta, v. 69, p. A319.

McClelland, W.C., and Mattinson, J.M., 1996, Resolving high precision U-Pb ages from Tertiary plutons with complex zircon systematics: Geochimica et Cosmochimica Acta, v. 60, p. 3955–3965, doi: 10.1016/0016-7037(96)00214-1.

McClelland, W.C., Gehrels, G.E., and Saleeby, J.B., 1992, Upper Jurassic–Lower Cretaceous basinal strata along the cordilleran margin: Implications for the accretionary history of the Alexander-Wrangellia-Peninsular terrane: Tectonics, v. 11, p. 823–835.

McCulloch, M.T., and Perfit, M.R., 1981, $^{143}Nd/^{144}Nd$, $^{87}Sr/^{86}Sr$ and trace element constraints on the petrogenesis of Aleutian island arc magmas: Earth and Planetary Science Letters, v. 56, p. 167–179, doi: 10.1016/0012-821X(81)90124-2.

Mehl, L., Hacker, B.R., and Hirth, G., 2001, Upper mantle deformation beneath intra-oceanic island arcs: The Talkeetna arc, south-central Alaska: Eos (Transactions, American Geophysical Union), v. 82, T41C–0878.

Mehl, L., Hacker, B.R., Hirth, G., and Kelemen, P.B., 2003, Arc-parallel flow within the mantle wedge: Evidence from the accreted Talkeetna arc, south central Alaska: Journal of Geophysical Research, v. 108, doi: 10.1029/2002JB002233.

Mundil, R., Ludwig, K.R., Metcalfe, I., and Renne, P.R., 2004, Age and timing of the Permian mass extinction: U/Pb dating of closed-system zircons: Science, v. 305, p. 1760–1763, doi: 10.1126/science.1101012.

Nokleberg, W.J., Jones, D.L., and Silberling, N.J., 1985, Origin and tectonic evolution of the Maclaren and Wrangellia terranes, eastern Alaska Range, Alaska: Geological Society of America Bulletin, v. 96, p. 1251–1270, doi: 10.1130/0016-7606(1985)96<1251:OATEOT>2.0.CO;2.

Nokleberg, W.J., Plafker, G., and Wilson, F.H., 1994, Geology of south-central Alaska, *in* Plafker, G., and Berg, H.C., eds., The geology of Alaska: Boulder, Colorado, Geological Society of America, Geology of North America, v. G-1, p. 311–366.

Onstott, T.C., Sisson, V.B., and Turner, D.L., 1989, Initial argon in amphiboles from the Chugach Mountains, southern Alaska: Journal of Geophysical Research, v. 94, p. 4361–4372.

Pavlis, T.L., 1982, Origin and age of the Border Ranges Fault of southern Alaska and its bearing on the late Mesozoic tectonic evolution of Alaska: Tectonics, v. 1, p. 343–368.

Pavlis, T.L., 1983, Pre-Cretaceous crystalline rocks of the western Chugach Mountains, Alaska: Nature of the basement of the Jurassic Peninsular terrane: Geological Society of America Bulletin, v. 94, p. 1329–1344, doi: 10.1130/0016-7606(1983)94<1329:PCROTW>2.0.CO;2.

Pavlis, T.L., Monteverde, D.H., Bowman, J.R., Rubenstone, J.L., and Reason, M.D., 1988, Early Cretaceous near-trench plutonism in southern Alaska: A tonalite-trondhjemite intrusive complex injected during ductile thrusting along the Border Ranges Fault system: Tectonics, v. 7, p. 1179–1199.

Pearce, J.A., Baker, P.E., Harvey, P.K., and Luff, I.W., 1995, Geochemical evidence for subduction fluxes, mantle melting and fractional crystallization beneath the south Sandwich Island arc: Journal of Petrology, v. 36, p. 1073–1109.

Plafker, G., Harris, A.G., and Reed, K.M., 1985, Early Pennsylvanian conodonts from the Strelna Formation, Chitina valley area, *in* Bartsch-Winkler, S., ed., The United States Geological Survey in Alaska: Accomplishments during 1984: U.S. Geological Survey Circular 967, p. 71–74.

Plafker, G., Nokleberg, W.J., and Lull, J.S., 1989, Bedrock geology and tectonic evolution of the Wrangellia, Peninsular, and Chugach terranes along the trans-Alaska crustal transect in the Chugach Mountains and south-

ern Copper River Basin, Alaska: Journal of Geophysical Research, v. 94, p. 4255–4295.

Reed, B.L., and Lanphere, M.A., 1973, Alaska-Aleutian Range Batholith: Geochronology, chemistry, and relation to circum-Pacific plutonism: Geological Society of America Bulletin, v. 84, p. 2583–2610, doi: 10.1130/0016-7606(1973)84<2583:ARBGCA>2.0.CO;2.

Richard, P., Shimizu, N., and Allègre, C.J., 1976, $^{143}Nd/^{146}Nd$, a natural tracer: An application to oceanic basalts: Earth and Planetary Science Letters, v. 31, p. 269–278, doi: 10.1016/0012-821X(76)90219-3.

Richter, D.H., and Jones, D.L., 1973, Structure and stratigraphy of the eastern Alaska Range, Alaska, *in* Pitcher, M.G., ed., Arctic geology: American Association of Petroleum Geologists Memoir 19, p. 408–420.

Ridgway, K.D., Trop, J.M., Nokleberg, W.J., Davidson, C.M., and Eastham, K.R., 2002, Mesozoic and Cenozoic tectonics of the eastern and central Alaska Range: Progressive basin development and deformation in a suture zone: Geological Society of America Bulletin, v. 114, p. 1480–1504, doi: 10.1130/0016-7606(2002)114<1480:MACTOT>2.0.CO;2.

Rioux, M., Kelemen, P., Mattinson, J., Hacker, B., and Blusztajn, J., 2004, Magmatic differentiation in the accreted Talkeetna arc, south-central Alaska: Eos (Transactions, American Geophysical Union), v. 85, V13B–1482.

Roeske, S., Mattinson, J., and Armstrong, R., 1989, Isotopic ages of glaucophane schists on the Kodiak Islands, southern Alaska, and their implications for the Mesozoic tectonic history of the Birder Ranges fault system: Geological Society of America Bulletin, v. 101, p. 1021–1037, doi: 10.1130/0016-7606(1989)101<1021:IAOGSO>2.3.CO;2.

Samson, S.D., Patchett, P.J., Gehrels, G.E., and Anderson, R.G., 1990, Nd and Sr isotopic characterization of the Wrangellia terrane and implications for crustal growth of the Canadian Cordillera: Journal of Geology, v. 98, p. 749–762.

Schmidt, J.M., Werdon, M.B., and Wardlaw, B., 2003, New mapping near Iron Creek, Talkeetna Mountains, indicates presence of Nikolai Greenstone, *in* Short notes on Alaskan geology 2003: Alaska Division of Geological and Geophysical Surveys Professional Report 120, p. 101–108.

Schoene, B., Crowley, J.L., Condon, D.J., Schmitz, M.D., and Bowring, S.A., 2006, Reassessing the uranium decay constants for geochronology using ID-TIMS U-Pb data: Geochimica et Cosmochimica Acta, v. 70, p. 426–445, doi: 10.1016/j.gca.2005.09.007.

Silberling, N.J., Jones, D.L., Monger, J.W.H., Coney, P.J., Berg, H.C., and Plafker, G., 1994, Lithotectonic terrane map of Alaska and adjacent parts of Canada, *in* Plafker, G., and Berg, H.C., eds., The geology of Alaska: Boulder, Colorado, Geological Society of America, Geology of North America, v. G-1, plate 3.

Sisson, V.B., and Onstott, T.C., 1986, Dating blueschist metamorphism: A combined $^{40}Ar/^{39}Ar$ and electron microprobe approach: Geochimica et Cosmochimica Acta, v. 50, p. 2111–2117, doi: 10.1016/0016-7037(86)90264-4.

Spera, F.J., and Bohrson, W.A., 2001, Energy-constrained open-system magmatic processes I: General model and energy-constrained assimilation and fractional crystallization (EC-AFC) formulation: Journal of Petrology, v. 42, p. 999–1018, doi: 10.1093/petrology/42.5.999.

Spera, F.J., and Bohrson, W.A., 2002, Energy-constrained open-system magmatic processes 3: Energy-constrained recharge, assimilation, and fractional crystallization (EC-RAFC): Geochemistry, Geophysics, Geosystems, v. 2, doi: 10.1029/2002GC000315.

Stacey, J.S., and Kramers, J.D., 1975, Approximation of terrestrial lead isotope evolution by a two-stage model: Earth and Planetary Science Letters, v. 26, p. 207–221, doi: 10.1016/0012-821X(75)90088-6.

Streckeisen, A., 1973, Plutonic rocks: Classification and nomenclature recommended by the IUGS Subcommission on the systematics of igneous rocks: Geotimes, v. 18, no. 10, p. 26–30.

Streckeisen, A., 1976, To each plutonic rock its proper name: Earth-Science Reviews, v. 12, p. 1–33, doi: 10.1016/0012-8252(76)90052-0.

Taylor, R.N., and Nesbitt, R.W., 1998, Isotopic characteristics of subduction fluids in an intra-oceanic setting, Izu-Bonin arc, Japan: Earth and Planetary Science Letters, v. 164, p. 79–98, doi: 10.1016/S0012-821X(98)00182-4.

Treloar, P.J., Petterson, M.G., Jan, M.Q., and Sullivan, M.A., 1996, A re-evaluation of the stratigraphy and evolution of the Kohistan arc sequence, Pakistan Himalaya: Implications for magmatic and tectonic arc-building processes: Geological Society [London] Journal, v. 153, p. 681–693.

Trop, J.M., Ridgway, K.D., Manuszak, J.D., and Layer, P., 2002, Mesozoic sedimentary-basin development on the allochthonous Wrangellia composite terrane, Wrangell Mountains basin, Alaska: A long-term record of terrane migration and arc construction: Geological Society of America Bulletin, v. 114, p. 693–717, doi: 10.1130/0016-7606(2002)114<0693:MSBDOT>2.0.CO;2.

Trop, J.M., Szuch, D.A., Rioux, M., and Blodgett, R.B., 2005, Sedimentology and provenance of the Upper Jurassic Naknek Formation, Talkeetna Mountains, Alaska: Bearings on the accretionary tectonic history of the Wrangellia composite terrane: Geological Society of America Bulletin, v. 117, p. 570–588, doi: 10.1130/B25575.1.

Turner, S., Hawkesworth, C., Rogers, N., Bartlett, J., Worthington, T., Hergt, J., Pearce, J., and Smith, I., 1997, ^{238}U-^{230}Th disequilibrium, magma petrogenesis, and flux rates beneath the depleted Tonga-Kermadec island arc: Geochimica et Cosmochimica Acta, v. 61, p. 4855–4884, doi: 10.1016/S0016-7037(97)00281-0.

Veizer, J., Ala, D., Azmy, K., Bruckschen, P., Buhl, D., Bruhn, F., Carden, G.A.F., Diener, A., Ebneth, S., Godderis, Y., Jasper, T., Korte, C., Pawellek, F., Podlaha, O.G., and Strauss, H., 1999, $^{87}Sr/^{86}Sr$, $\delta^{13}C$ and $\delta^{18}O$ evolution of Phanerozoic seawater: Chemical Geology, v. 161, p. 59–88, doi: 10.1016/S0009-2541(99)00081-9.

Wendt, I., and Carl, C., 1991, The statistical distribution of the mean squared weighted deviation: Chemical Geology, v. 86, p. 275–285.

Wilson, F.H., Dover, J.H., Bradley, D.C., Weber, F.R., Bundtzen, T.K., and Haeussler, P.J., 1998, Geologic map of central (interior) Alaska: U.S. Geological Survey Open-File Report 98-133, 63 p.

Winkler, G.R., 1992, Geologic map and summary geochronology of the Anchorage 1° × 3° quadrangle, southern Alaska: U. S. Geological Survey Miscellaneous Investigation Series Map I-2283.

Winkler, G.R., Silberman, M.L., Grantz, A., Miller, R.J., and MacKevett, E.M., Jr., 1981, Geologic map and summary geochronology of the Valdez quadrangle, southern Alaska: U.S. Geological Survey Open-File Report 80-892, scale 1:250,000.

Woodhead, J.D., 1989, Geochemistry of the Mariana arc (western Pacific): Source composition and processes: Chemical Geology, v. 76, p. 1–24, doi: 10.1016/0009-2541(89)90124-1.

Manuscript received 9 January 2006
Revised manuscript received 22 November 2006
Manuscript accepted 31 January 2007

Printed in the USA